Microwave Remote Sensing:
2. Theory, Algorithms and Applications

Dr. Fuzhong Weng
Sensor Physics Branch
Center for Satellite Applications and Research
National Environmental Satellites, Data and Information Service
National Oceanic and Atmospheric Administration

2009 Update

Outline

- **Microwave Remote Sensing Theory**
  - MW gas spectrum
  - Radiative Transfer Approximation
- **Microwave Algorithms**
  - Cloud liquid water
  - Cloud ice water
  - Precipitation
  - Temperature and water vapor
- **Product Applications**
  - Model validation and intercomparison
  - NWP model validations
  - Climate monitoring and trending

Microwave Absorption Spectrum

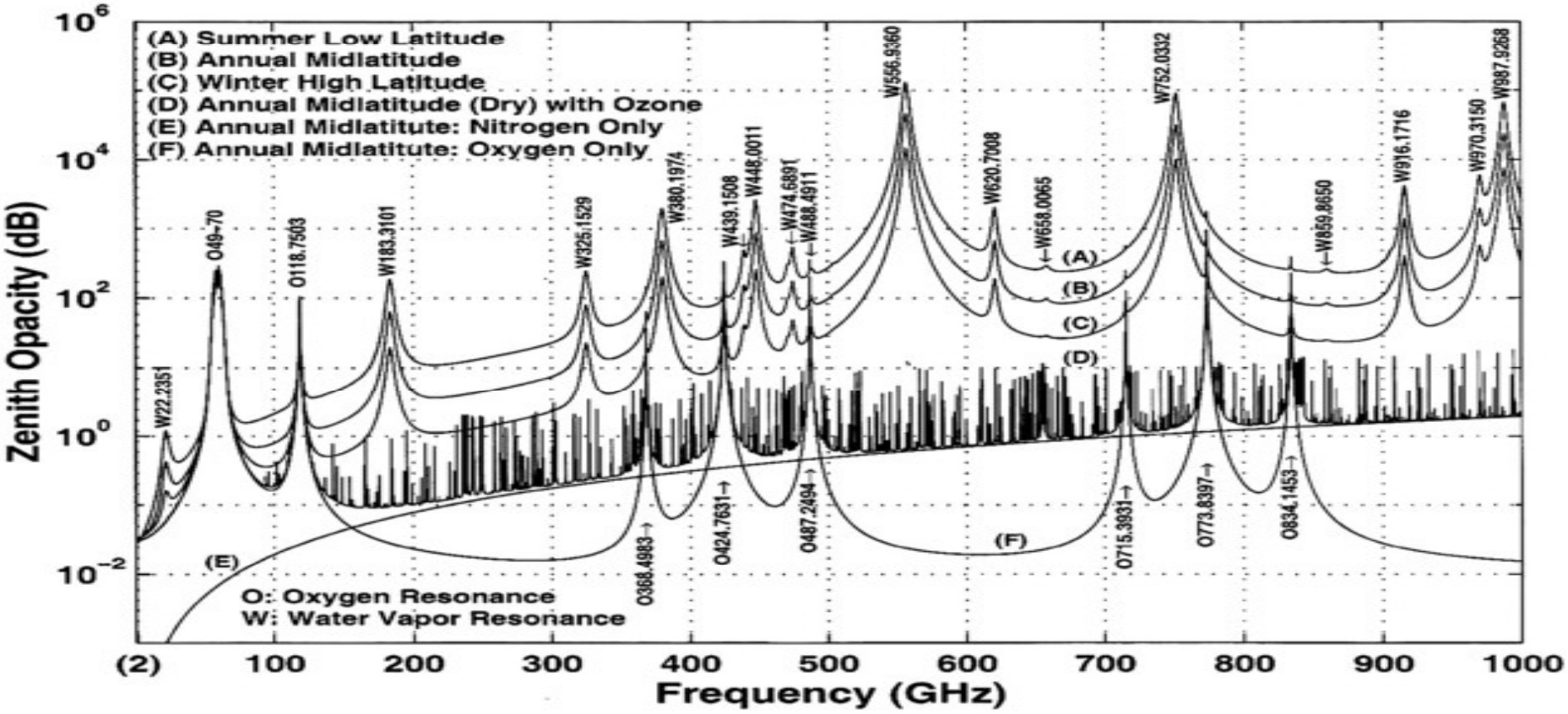

Janssen M. A., 1993: Atmospheric remote sensing by microwave radiometry, Chapter 2, John Wiley &Son inc

1. Rotational transition line: O3,H2O,CO,ClO, N2O…
2. Spin-rotational transition: O2 and zeeman splitting in upper atmosphere where geomagnetic field is important
3. Doppler and pressure broading

Microwave Penetration Depth

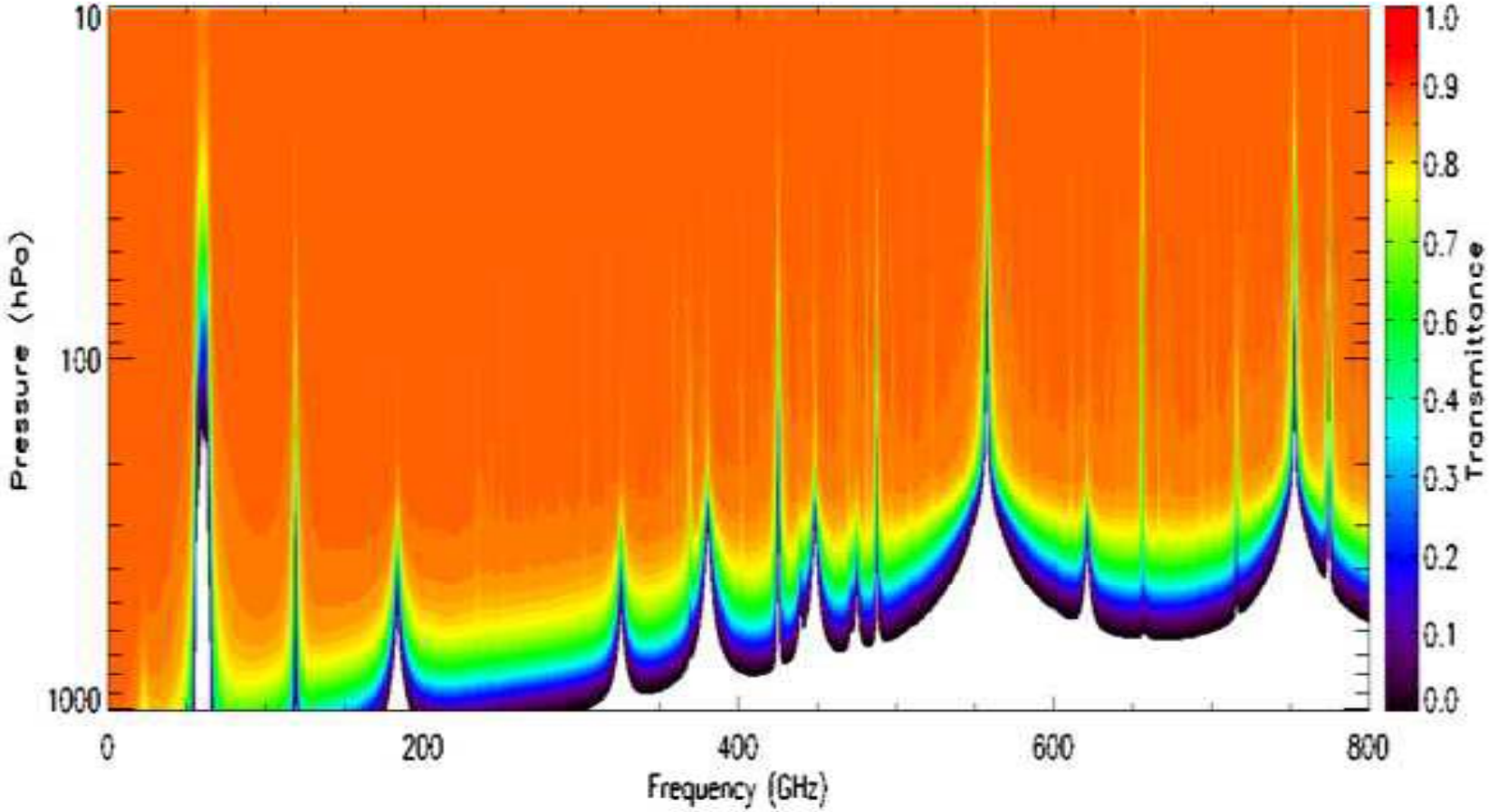

Instrument Spectrum Allocations

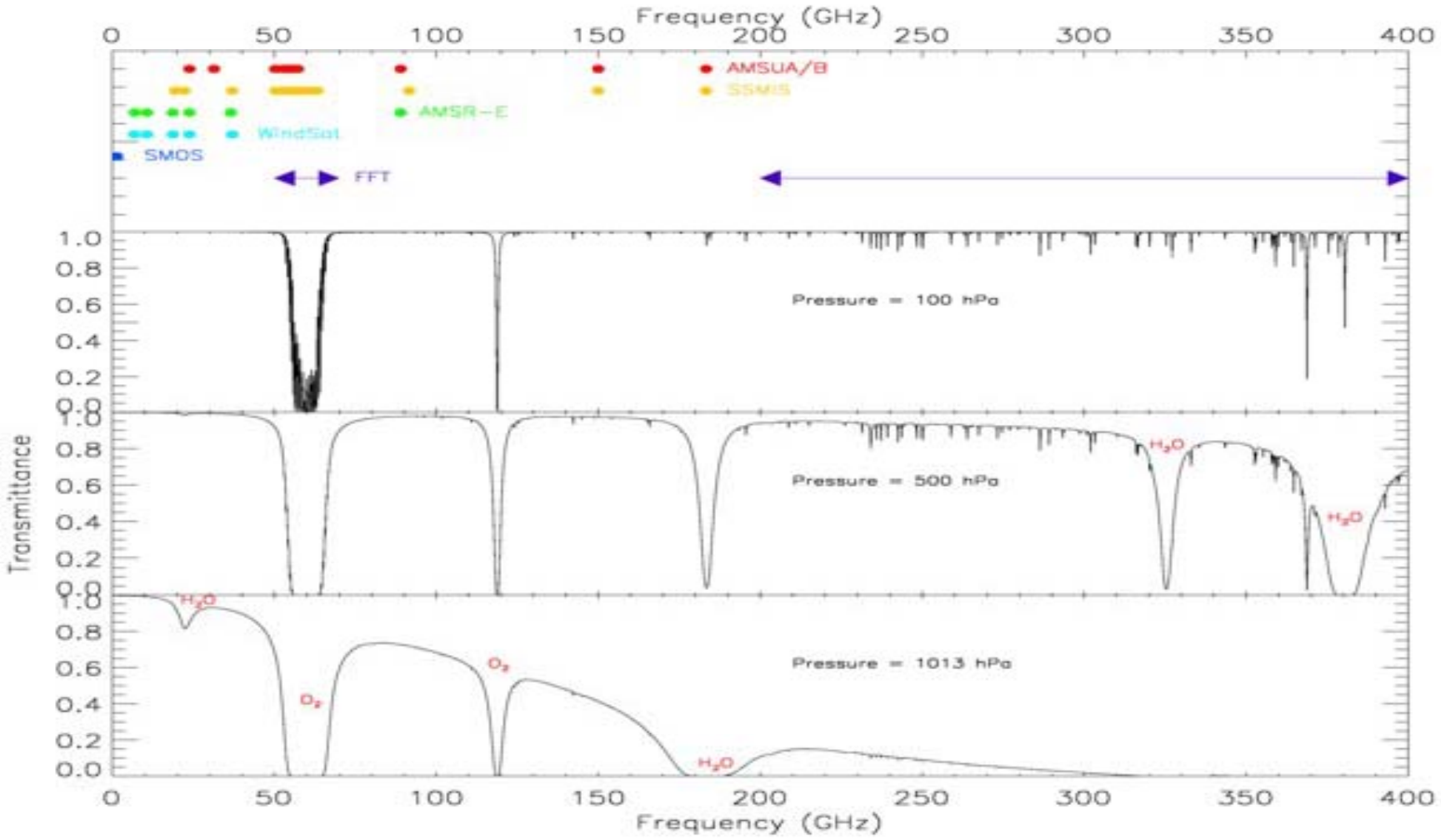

MW Stratosphere and Mesosphere Sounding

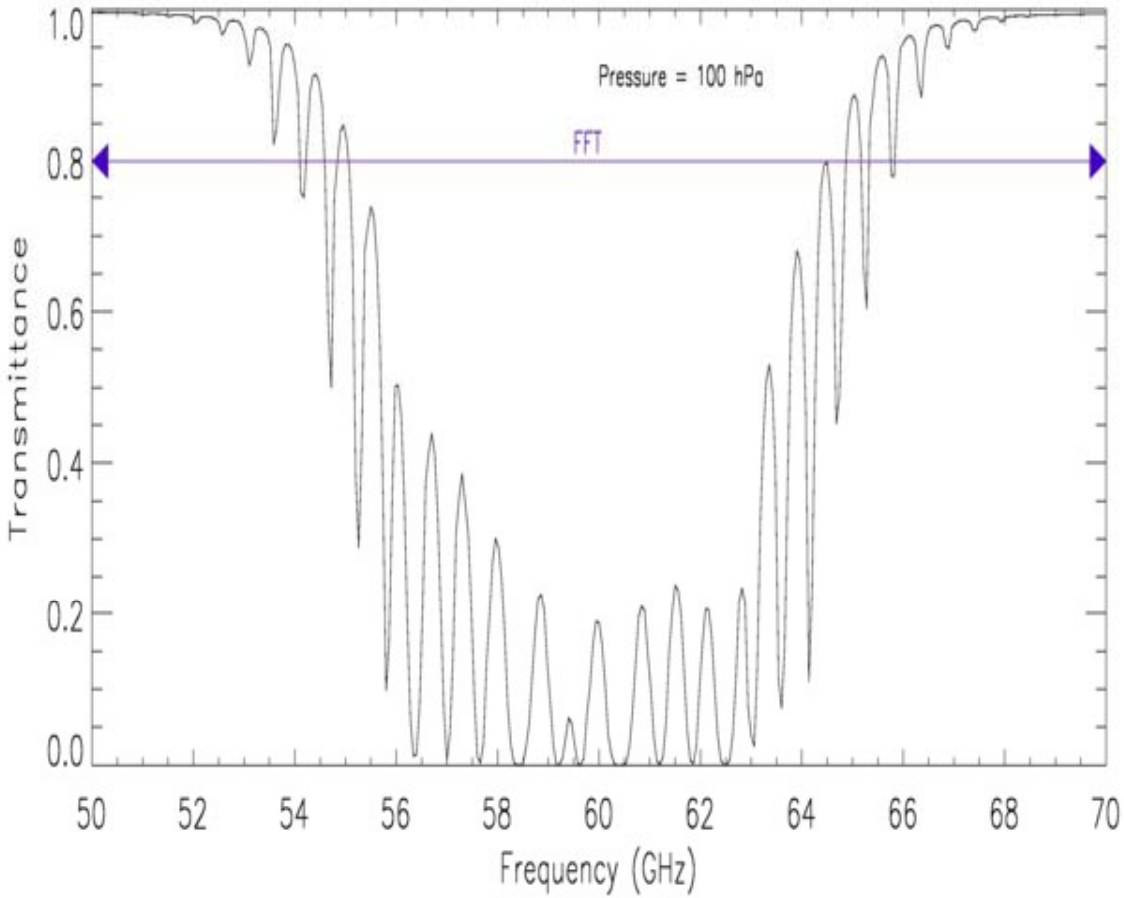

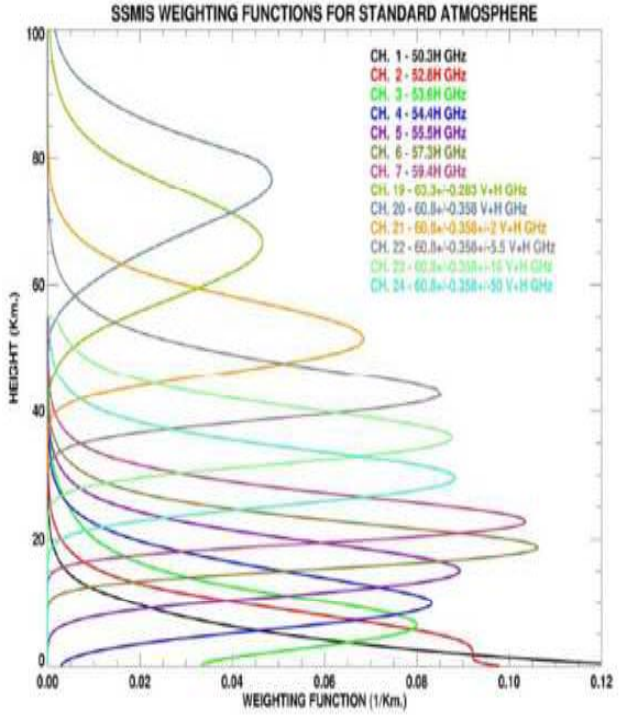

Figure 7.2: SSMIS Weighting function

Millimeter Wavelength Spectroscopy

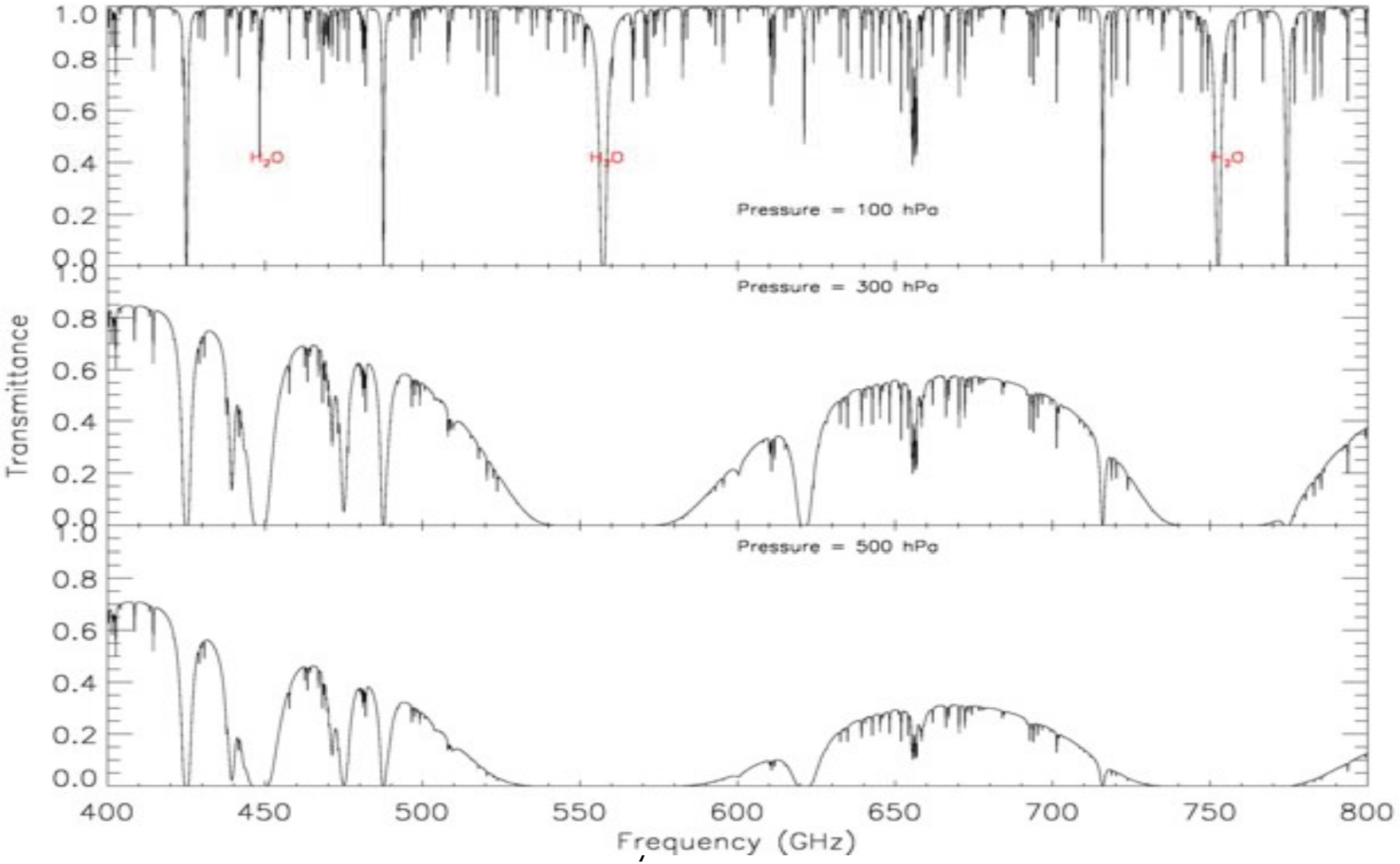

Global Land Emissivity Characterization
SSM/I Fifteen Year Time Series

- Large season change at higher frequencies
- Large polarization difference for several surfaces (e.g. desert, snov flooding)
- Deserts appear as a scattering medium

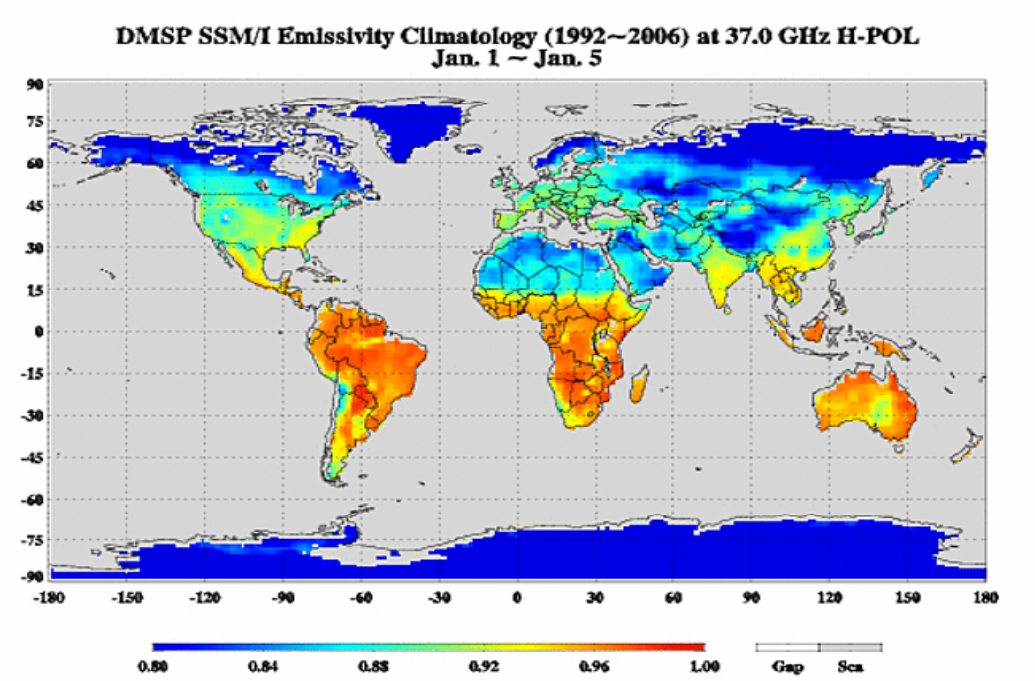

SSM/I surface emissivity climatological data set is developed at various time scales (e.g. pentad, weekly and monthly, anomaly). SSM/I sensors from F10 to 15 satellites are intercalibrated to a reference satellite (F13)

Microwave Surface Emissivity Spectra

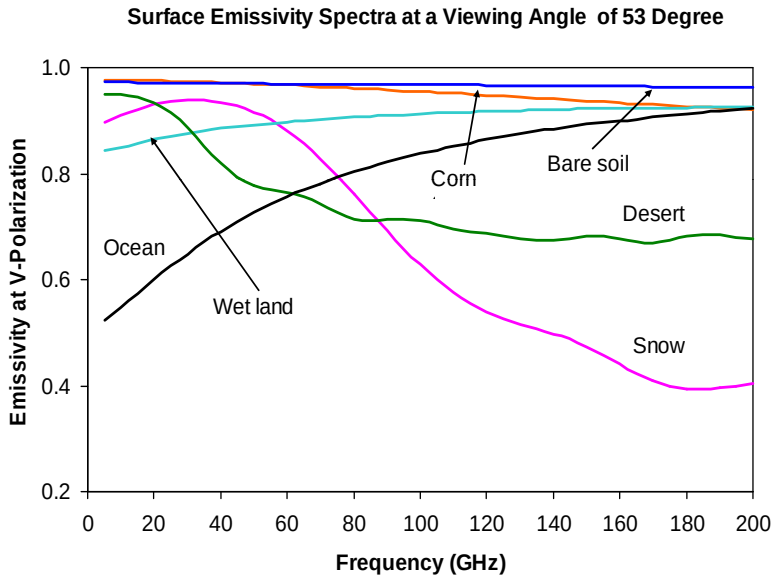

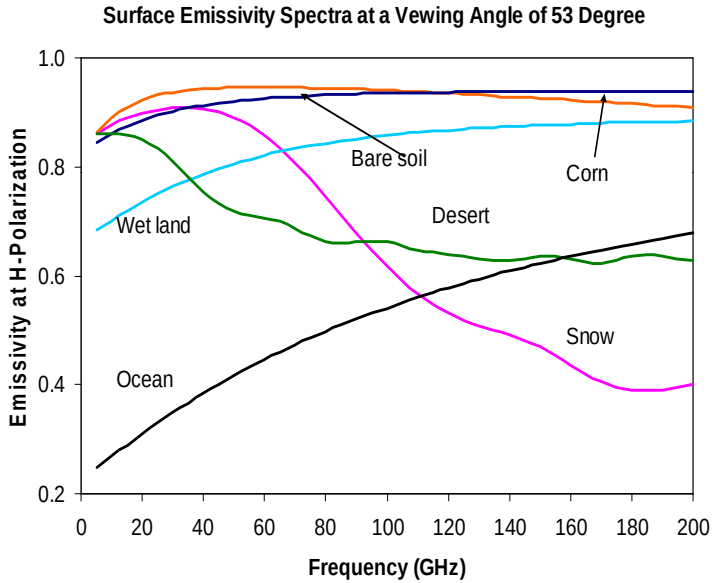

Advanced Microwave Sounding Unit

Imaging and Temperature Sounding Channels

23.8 GHz

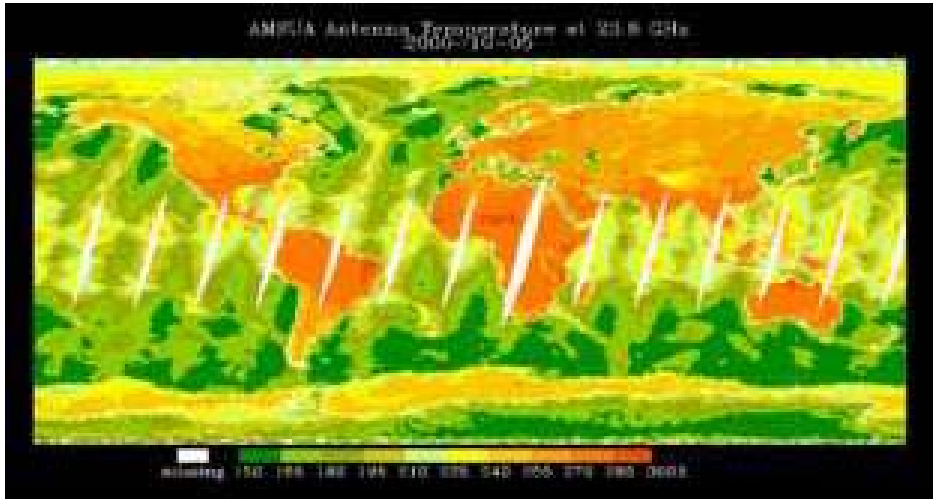

31.4 GHz

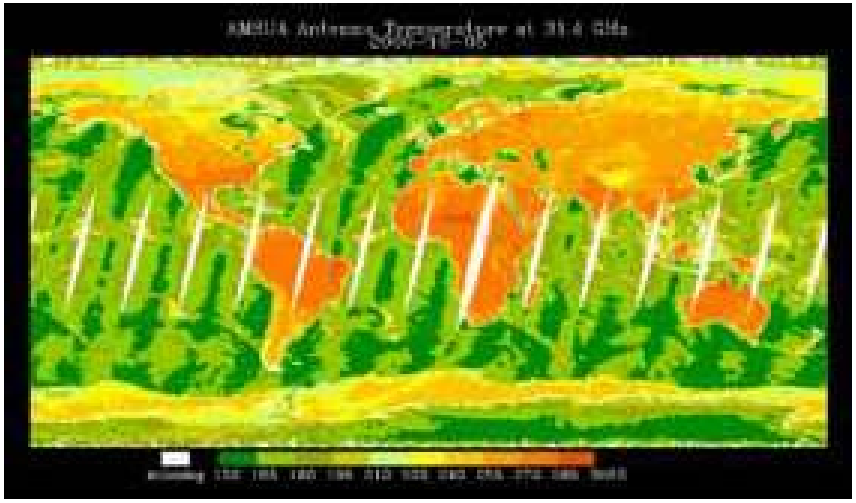

52.8 GHz

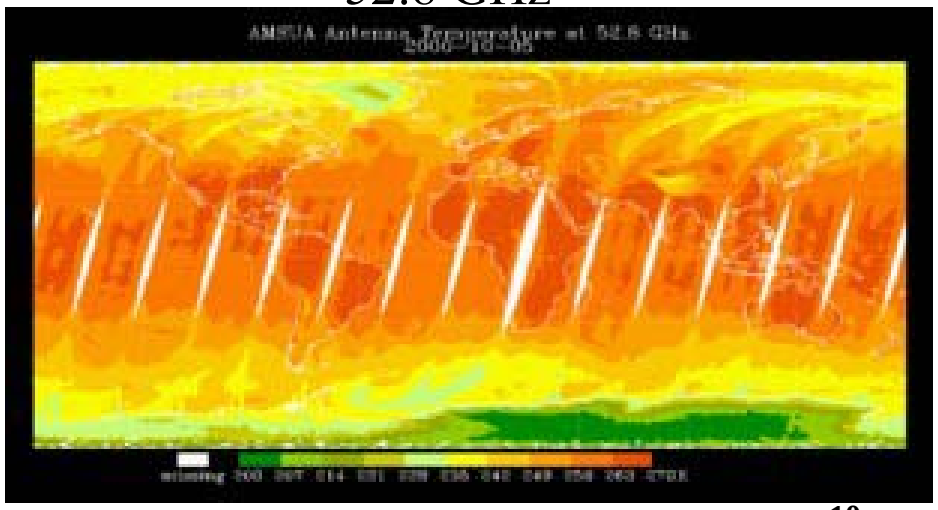

53.7 GHz

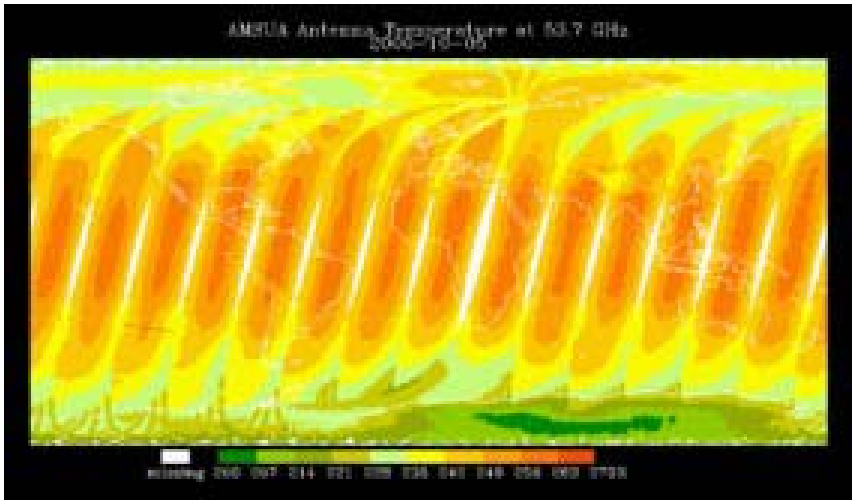

Advanced Microwave Sounding Unit

Imaging and Moisture Sounding Channels

89 GHz

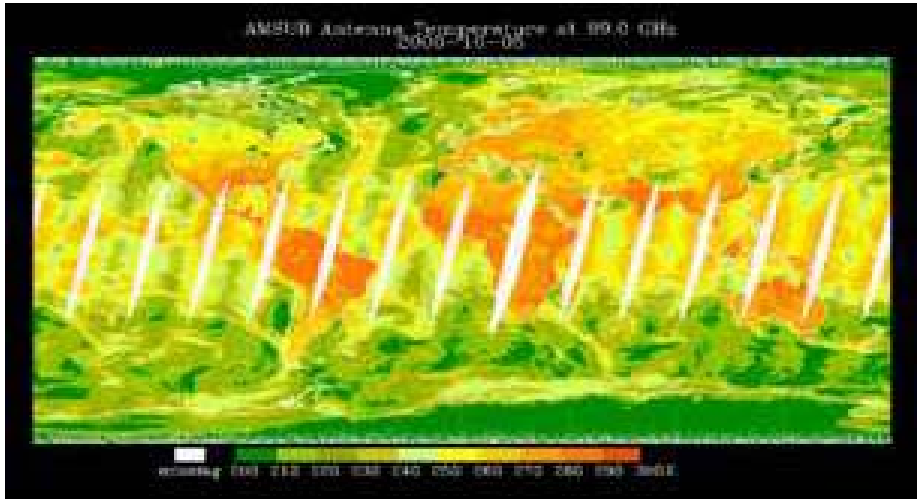

183±3 GHz

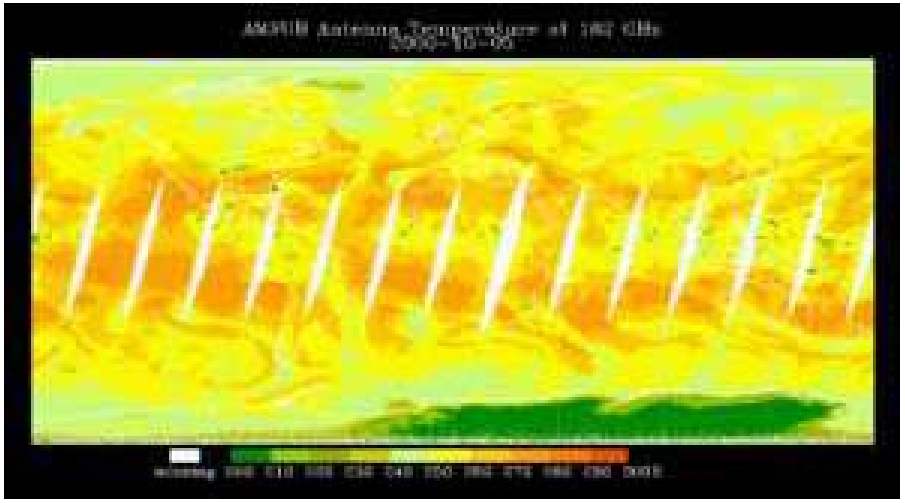

150 GHz

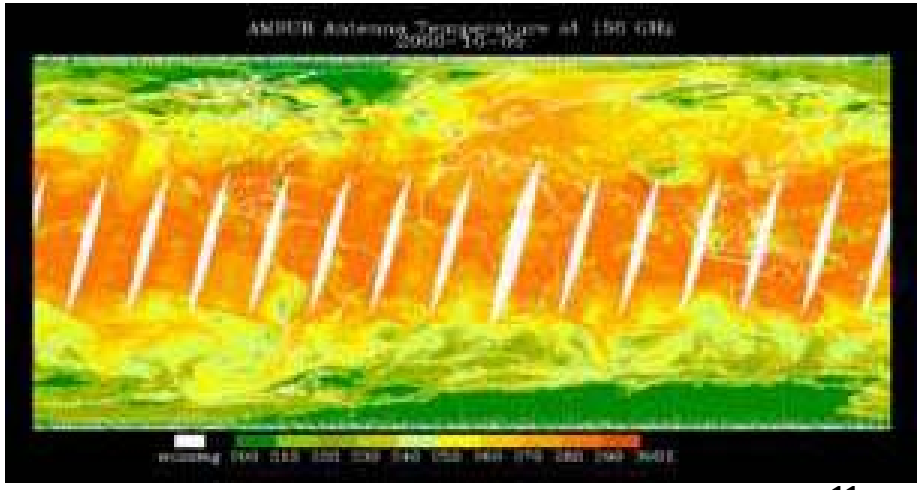

183± 1 GHz

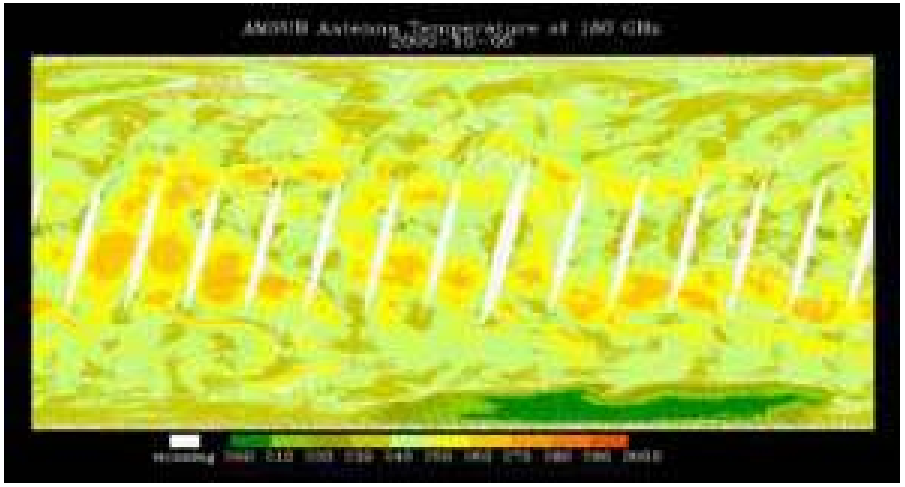

Outline

- **Microwave Remote Sensing Theory**
  - MW gas spectrum
  - Radiative Transfer Approximation
- **Microwave Algorithms**
  - Cloud liquid water
  - Cloud ice water
  - Precipitation
  - Temperature and water vapor
- **Product Applications**
  - Model validation and intercomparison
  - NWP model validations
  - Climate monitoring and trending

Microwave Remote Sensing of Clouds

- A large contrast exists between cloudy and "clear" conditions, thanks to low ocean emissivity.
- Brightness temp increases exponentially with liquid water, thus requiring a logarithmic function for linearization
- "The linear regime" is dependent on frequency. We can meet more customer's needs (e.g. rain water..) if the measurements at each frequency are optimally utilized in the retrievals

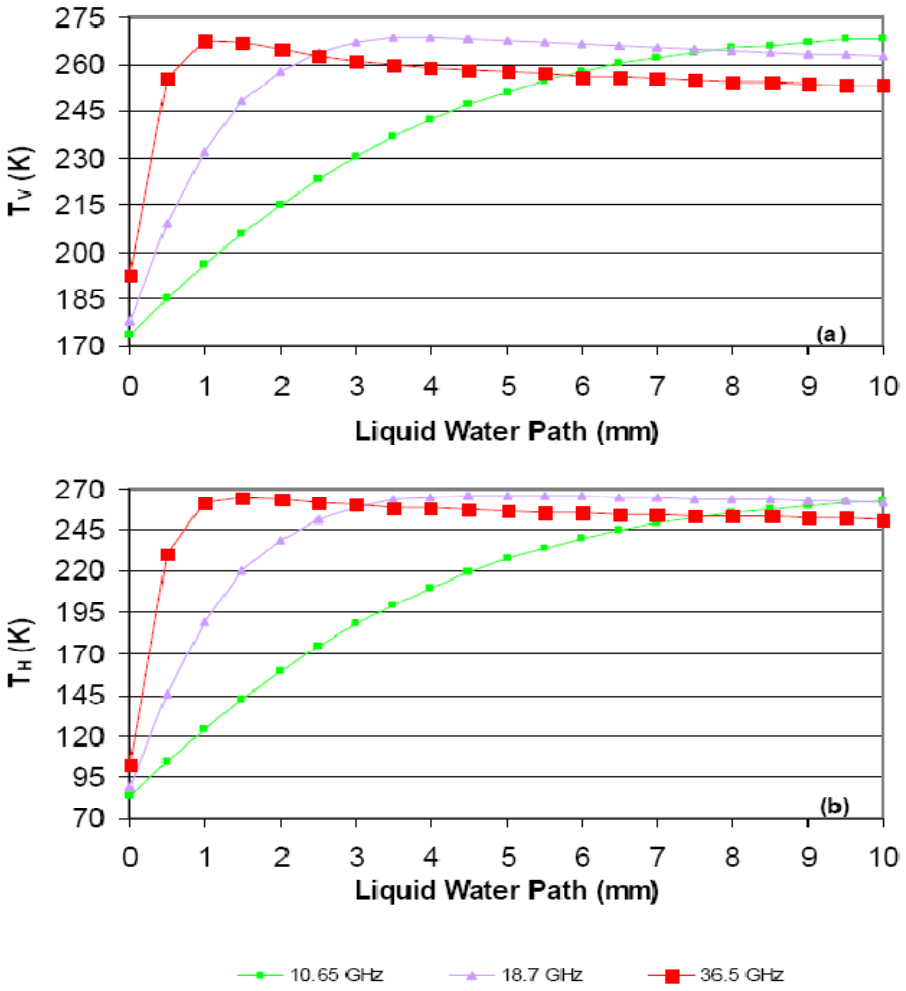

Emission Approach

3.3 Radiative Transfer Approximation

3.3.1 Emission-Based Model

Microwave radiative transfer can be simplified if single and multiple scattering terms are neglected and there is no azimuthally dependent terms are included. Thus, in Eq. 3.17, we can derive

$$\mu \frac{d\mathbf{I}(\tau,\mu)}{d\tau} = \mathbf{I}(\tau,\mu) - \mathbf{B}(\tau), \tag{3.21}$$

where $\mathbf{I}$ is the zeroth order term of radiance in the cosine mode in Eq.3.17. For convenience, we neglect the subscript of Fourier zeroth component. when the terms from single and multiple scattering are neglected and scattering. After the integration term disappears, the solution of radiance vector can be expressed in a form (Liou, 1980)

$$\begin{aligned}\mathbf{I}(\tau_0,\mu) = {} & \mathbf{I}(\tau_s,\mu)\exp(-\tau_s/\mu) + \\ & \int_0^1 \mathbf{r_s}(\mu,\mu')d\mu' \int_{\tau_0}^{\tau_s} \mathbf{B}(\tau,T)\exp[-\frac{(\tau-\tau_0)}{\mu'}]d\tau/\mu + \\ & \int_{\tau_s}^{\tau_0} \mathbf{B}(\tau,T)\exp[-\frac{(\tau_s-\tau)}{\mu}]d\tau/\mu,\end{aligned} \tag{3.22}$$

or

$$\mathbf{I}(\tau_0,\mu) = \mathbf{I}(\tau_s,\mu)\exp(-\tau_s/\mu) + \mathbf{I_u} + \mathbf{I_d}, \tag{3.23}$$

$$\begin{aligned}\mathbf{I_u} &= \int_{\tau_s}^{\tau_0} \mathbf{B}(\tau,T)\exp[-\frac{(\tau_s-\tau)}{\mu}]d\tau,/\mu \\ \mathbf{I_d} &= \int_0^1 \mathbf{r_s}(\mu,\mu')d\mu' \int_{\tau_0}^{\tau_s} \mathbf{B}(\tau,T)\exp[-\frac{(\tau-\tau_0)}{\mu'}]d\tau/\mu\end{aligned} \tag{3.24}$$

Emission-Based RT Model (1/3)

At the microwave frequencies, radiance is related to brightness temperature under Rayleigh-Jean approximation. Also, we only consider the first Stokes component (i.e. intensity), which is the brightness temperature. After some manipulation, we can derive

$$
\begin{aligned}
T_b &= \epsilon T_s \exp(-\tau_s/\mu) + T_u + (1-\epsilon)(1+\Omega)(T_d + T_c)\exp(-\tau_s/\mu), \quad (3.25)\\
T_d &= \int_{\tau_0}^{\tau_s} B(\tau,T)\exp(-\frac{(\tau-\tau_0)}{\mu})d\tau/\mu,\\
T_u &= \int_{\tau_s}^{\tau 0} B(\tau,T)\exp(-\frac{(\tau_s-\tau)}{\mu})d\tau/\mu,
\end{aligned}
\quad (3.26)
$$

where ϵ is the surface emissivity and T_s is the surface temperature, and T_c is the cosmic background brightness temperature. The parameter, Ω, is introduced for non-specular effect of surface reflection and varies with surface roughness, sea surface wind speed, frequency, and atmospheric transmittance (Wentz, 1998). Eq. 5.1 has been so far widely used for retrieving surface emissivity assume other components such as T_s, upwelling and downwelling brightness temperatures are estimated from other means (Weng et al., 2000; Prigent, 2004).

Emission-Based RT Model (2/3)

For an isothermal atmosphere, upwelling and downwelling components in terms of brightness temperatures can be approximated as

$$\begin{aligned} T_u &\approx T_d \\ &\equiv (1-\Upsilon)T_m, \end{aligned} \tag{3.27}$$

where $\Upsilon = \exp(-\frac{(\tau_s-\tau_0)}{\mu})$ and T_m is the atmospheric temperature. Thus,

$$T_b = T_s[1-(1-\epsilon)\Upsilon^2] - \Delta T(1-\Upsilon)[1+(1-\epsilon)\Upsilon], \tag{3.28}$$

where $\Delta T = T_s - T_m$. It is apparent that brightness temperatures under these approximation is directly related by the layer mean temperature and atmospheric transmittance. When emissivity is low (0.9), brightness temperature increases as atmospheric transmittance (more cloud and water vapor) decreases (see Fig. 3.3.1. This is why over oceans clouds having liquid water increases brightness temperature and are easily detected from lower microwave measurements. Eq. 5.4 can be analytically used to retrieve cloud liquid water path when ΔT is very small.

Emission-Based RT Model (3/3)

In an absence of scattering, brightness temperatures can be linearly a function of cloud liquid water path (L) and precipitable water path (V) (Weng et al. 2003) by further assuming an isothermal atmosphere in Eq. 5.4 and a Rayleigh scattering for liquid-phase droplets Eq. 3.44, i.e.,

$$T_b = T_s[1-(1-\epsilon)\Upsilon^2], \tag{6.1}$$

where ϵ and T_s are surface emissivity and temperature, respectively, and

$$\Upsilon = \exp[-(\tau_O + \tau_V + \tau_L)/\mu)] \tag{6.2}$$

where τ_O, τ_V and τ_L are the optical thicknesses of oxygen, water vapor and liquid respectively.

$$\tau_L = \int_{\Delta Z} \kappa^{Ray} LWC dz \tag{6.3}$$

where

$$\kappa^{Ray} = \frac{6\pi}{\lambda\rho_w} Im\left\{\frac{m^2-1}{m^2-2}\right\} \tag{6.4}$$

and

$$\tau_V = \int_0^{\infty} \kappa^{H_2O}\rho_V dz \tag{6.5}$$

where κ_{H_2O} is the mass absorption coefficient of water vapor having a unit of m^2/kg, and ρ_v is the water vapor density in atmosphere. Lets assume κ^{Ray} and κ^{H_2O} are independent of height. Then, we have

$$\tau_L = \kappa_L L \tag{6.6}$$

Why MW can't "see" cloud well over land?

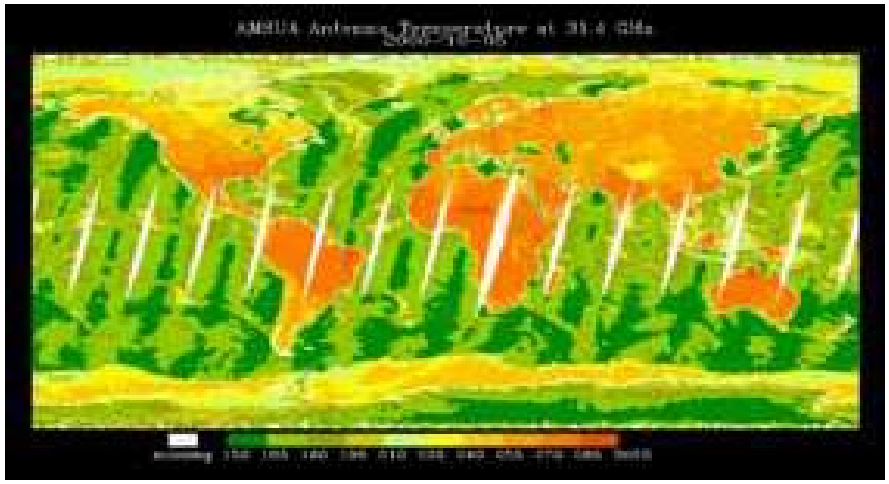

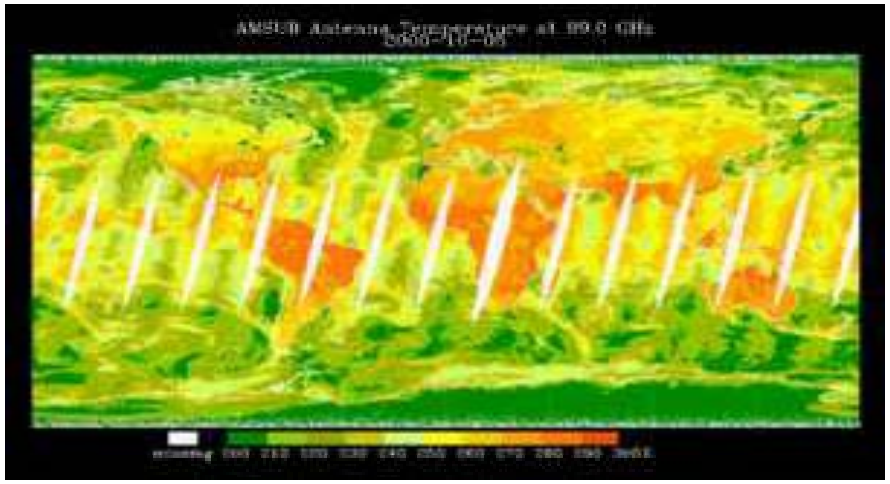

$$\frac{\partial T_b}{\partial L} = -2T_e(1-\varepsilon)\tau \frac{\partial \tau}{\partial L}$$

Liquid Water Absorption

where κ_L is the mass absorption coefficient of liquid-phase cloud, viz,

$$\kappa_L = \frac{6\pi}{\lambda \rho_w} Im \left\{ \frac{m^2 - 1}{m^2 + 2} \right\}, \tag{6.7}$$

Here, we use a different notation to indicate there is a further approximation being made for cloud absorption coefficient which can be derived from a mean cloud temperature in the complex dielectric constant. And, we also have

$$\tau_V = \kappa_V V \tag{6.8}$$

where

$$V = \int_0^\infty \rho_V dz \tag{6.9}$$

and

$$L = \int_{\Delta Z} LWC dz \tag{6.10}$$

are the vertically integrated water vapor and liquid water, respectively. Thus, atmospheric transmittance becomes

$$\Upsilon = \exp[-(\tau_O + \kappa_V V + \kappa_L L)/\mu) \tag{6.11}$$

Scattering Approach: 2 Streams Approximation

3.3.2 Scattering-Based Model

For a scattering and absorbing atmosphere, the radiance may be considered azimuthally independent so that the radiative transfer equation is given as

$$\mu \frac{dI(\tau,\mu)}{d\tau} = I(\tau,\mu) - \frac{\omega(\tau)}{2}\int_{-1}^{1} P(\mu,\mu')I(\tau,\mu')d\mu' - (1-\omega(\tau))B(T) \quad (3.29)$$

where I is the radiance; $\omega(\tau)$ the single-scattering albedo; $P(\mu,\mu')$ the phase function; $B(T)$ the Planck function; T the thermal temperature; τ the optical thickness; μ the cosine of incident zenith angle and μ' the cosine of scattering zenith angle.

A solution for Eq. (??) was derived at arbitrary viewing angles using a two-stream approximation (Weng and Grody, 2000),

$$\mu \frac{dI(\tau,\mu)}{d\tau} = [1-\omega(1-b)]I(\tau,\mu) - \omega b I(\tau,-\mu) - (1-\omega)B, \quad (3.30)$$

$$-\mu \frac{dI(\tau,-\mu)}{d\tau} = [1-\omega(1-b)]I(\tau,-\mu) - \omega b I(\tau,\mu) - (1-\omega)B, \quad (3.31)$$

where b and $1-b$ is the ratio of the integrated scattering energy in the backward and forward directions, respectively. For an isotropic scattering, $b = 1/2$ so that the scattered energy is the same in both directions. Since b is generally less than $1/2$, forward scattering is much stronger than backward scattering and the resulting upwelling radiation is reduced.

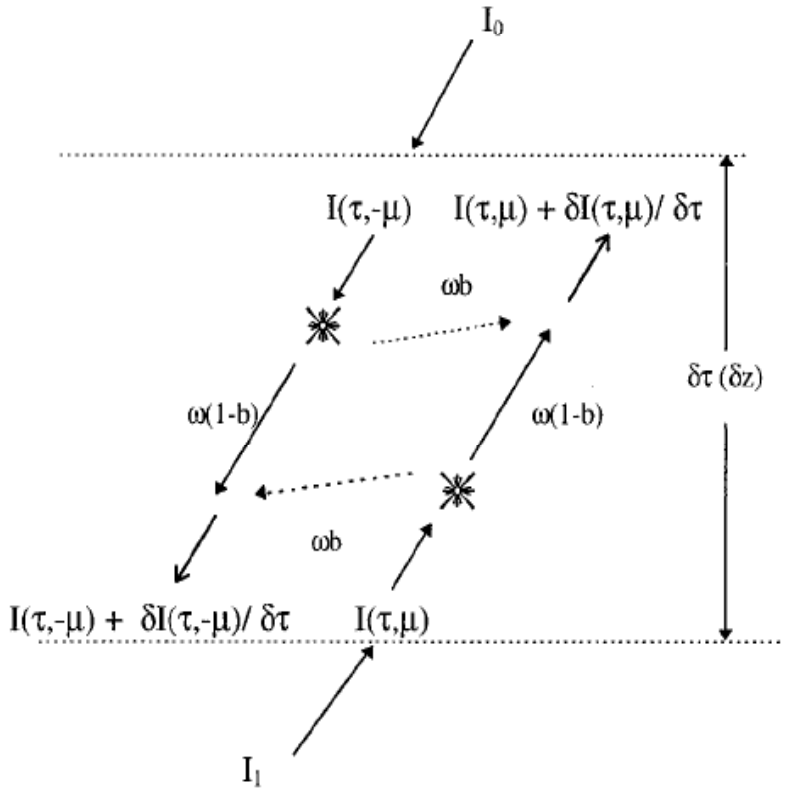

FIG. 1. A schematic diagram of the two-stream radiative transfer in an ice cloud layer.

Two-Stream Model Solution

Equations (3.30) and (3.31) can be combined into two decoupled second order differential equations with constant coefficients, assuming that ω, b and B are independent of τ. These equations can be used to analyze the scattering from the atmosphere or surface. The upwelling radiance observed from satellites for an ice cloud layer is derived by neglecting reflections at the cloud top and bottom (Weng and Grody, 2000). However, for surfaces such as snow, the upwelling radiance is modified by the reflectivity and transmissivity at the upper boundary where a discontinuity in the dielectric constant occurs (see Fig. 1). As a result, the solutions for the upwelling and downwelling radiance are

$$I(\tau,\mu) = \frac{I_0'[\gamma_1 e^{\kappa(\tau-\tau_1)} - \gamma_2 e^{-\kappa(\tau-\tau_1)}] - I_1'[\beta_3 e^{\kappa(\tau-\tau_0)} - \beta_4 e^{-\kappa(\tau-\tau_0)}]}{\beta_1\gamma_4 e^{-\kappa(\tau_1-\tau_0)} - \beta_2\gamma_3 e^{\kappa(\tau_1-\tau_0)}} + B \tag{3.32}$$

$$I(\tau,-\mu) = \frac{I_0'[\gamma_4 e^{\kappa(\tau-\tau_1)} - \gamma_3 e^{-\kappa(\tau-\tau_1)}] - I_1'[\beta_2 e^{\kappa(\tau-\tau_0)} - \beta_1 e^{-\kappa(\tau-\tau_0)}]}{\beta_1\gamma_4 e^{-\kappa(\tau_1-\tau_0)} - \beta_2\gamma_3 e^{\kappa(\tau_1-\tau_0)}} + B \tag{3.33}$$

where κ is the eigenvalue in solving the differential equations and related to particle optical parameters. Also, $I_1' = I_1 - B(1-R_{23})$; $I_0' = I_0(1-R_{12}) - B(1-R_{21})$, where I_1 is the upwelling radiance at $\tau = \tau_1$ from the bottom layer and I_0 is the downwelling radiance at $\tau = \tau_0$ from the top layer. The

Algorithms of Cloud (Rain) Liquid Water Path: Vertically Integrated Liquid Water over Unit Area

Cloud Liquid Water Algorithm

$$\kappa_V V + \kappa_L L = -\frac{\mu}{2}\left\{\ln(T_s - T_b) - \ln[T_s(1-\epsilon)] + \frac{2\tau_{O_2}}{\mu}\right\} \quad (6$$

Using two channel measurements, we can derive

$$L = a_0\mu[\ln(T_s - T_{b,1}) - a_1\ln(T_s - T_{b,2}) - a_2], \quad (6$$

and

$$V = b_0\mu[\ln(T_s - T_{b,1}) - b_1\ln(T_s - T_{b,2}) - b_2], \quad (6.14)$$

respectively. $T_{b,1}$ is the channel sensitive to liquid and $T_{b,2}$ is the channel sensitive to water vapor. The coefficients, $a_{0,1,2}$ and $b_{0,1,2}$ are related to water vapor and liquid water mass absorption coefficients as

$$a_0 = -0.5\kappa_{V2}/(\kappa_{V2}\kappa_{L1} - \kappa_{V1}\kappa_{L2}) \quad (6.15)$$

$$b_0 = 0.5\kappa_{L2}/(\kappa_{V2}\kappa_{L1} - \kappa_{V1}\kappa_{L2}) \quad (6.16)$$

$$a_1 = \kappa_{V1}/\kappa_{V2} \quad (6.17)$$

$$b_1 = \kappa_{L1}/\kappa_{L2} \quad (6.18)$$

$$a_2 = -2(\tau_{O,1} - a_1\tau_{O,2})/\mu + (1-a_1)\ln[T_s(1-\epsilon_1)] - a_1\ln(1-\epsilon_2) \quad (6.19)$$

$$b_2 = -2(\tau_{O,1} - b_1\tau_{O,2})/\mu + (1-b_1)\ln[T_s(1-\epsilon_1)] - b_1\ln(1-\epsilon_2) \quad (6.20)$$

From Rayleigh's approximation, κ_L can be parameterized as a function of cloud layer temperature, T_L in Celsius as

$$\kappa_L - a_L + b_L T_L + C_L T_L^2, \quad (6.21)$$

Oxygen optical thickness is parameterized as a function of sea surface temperature through

$$\tau_O = a_o + b_o T_s, \quad (6.22)$$

Table 6.1: The parameters calculated at four AMSU-A channels and used in liquid water and water vapor path algorithms

	23.8 GHz	31.4 GHz	50.3 GHz	89 GHz
κ_V	4.80423E-3	1.93241E-3	3.76950E-3	1.15839E-2
κ_L - a_L	1.18201E-1	1.98774E-1	4.53967E-3	1.03486E00
κ_L - b_L	-3.48761E-3	-5.45692E-3	-9.68548E-3	-9.71510E-3
κ_L - c_L	5.01301E-5	7.18339E-5	8.57815E-5	-6.59140E-5
τ_O-a_o	3.21410E-2	5.34214E-2	6.26545E-1	1.08333E-1
τ_O-b_o	-6.31860E-5	-1.04835E-4	-1.09961E-3	-2.21042E-4

Sometime, satellite measurements under clear condition can be used to derive some coefficients. From Eq. 6.13, set L=0

Cloud Liquid Water Algorithm Evolution

$$LWP = a_0\left[\ln(T_s - TB_1) - a_1 - a_2\ln(T_s - TB_2)\right]$$
$$TPW = b_0\left[\ln(T_s - TB_1) - b_1 - b_2\ln(T_s - TB_2)\right]$$

Statistical: all coefficients are from simulated data sets & Ts=290

$$\ln(290 - TB_1) = a_1 + a_2\ln(290 - TB_2)$$

Semi–Physical: a0 is derived from simulated data set, a1 and a2 are from microwave measurements under clear conditions

a0 = -0.5κv23 / (κv23κl31 - κv31κl23)
b0 = 0.5κl23 / (κv23κl31 - κv31κl23)
a1 = κv31 / κv23; b1 = κl31 / κl23
a2 = - 2.0(τo31 - a1 τo23) / μ + (1.0 - a1) ln(Ts) + ln(1.0 - ε31) – a1 ln(1.0 - ε23)
b2 = - 2.0(τo31 - b1 τo23) / μ + (1.0 - b1)ln(Ts) + ln(1.0 - ε31) – b1 ln(1.0 -ε23)

Physical: all coefficients are derived as function of cloud layer temp, surface wind speed, & surface temp

$$TB = B[1-(1-\varepsilon)e^{-2\tau_1/\mu}] - [B(T_s) - B(T)](1-e^{-\tau_1/\mu})[1+(1-\varepsilon)e^{-\tau_1/\mu}]$$

Emissision-Based

Physical: Microwave integrated Retrieval system, 1dvarwith scattering all hydrometeors profiles

$$J = \frac{1}{2}\left(\mathbf{x}-\mathbf{x}^b\right)^T\mathbf{B}^{-1}\left(\mathbf{x}-\mathbf{x}^b\right) + \frac{1}{2}\left[\mathbf{I}(\mathbf{x})-\mathbf{I}^o\right]^T(\mathbf{E}+\mathbf{F})^{-1}\left[\mathbf{I}(\mathbf{x})-\mathbf{I}^o\right]$$

$$\mu\frac{d\mathbf{I}(\tau,\mu,\phi)}{d\tau} = -\mathbf{I}(\tau,\mu,\phi) + \frac{\varpi}{4\pi}\int_0^{2\pi}\int_{-1}^{1}\mathbf{M}(\tau;\mu,\phi;\mu',\phi')\mathbf{I}(\tau,\mu',\phi')d\mu'd\phi' + \mathbf{S}(\tau,\mu,\phi;\mu_0,\phi_0)$$

Scattering Based

SSM/I Cloud Liquid Water Algorithm: Operational at FNMOC and NESDIS

Pros:

- ***Semi-Physical with easy understanding***
- ***Large dynamic range (rain and non-rain)***
- ***Clean background due to uses of real measurements***
- ***Validated with ASTEX data for non-raining clouds***

Cons:

- ***Difficult to accommodate information from new channels and ancillary data***
- ***Cloud layer temp is implicit***

$$\mathrm{LWP} = \begin{cases} \mathrm{LWP}_{19V} & \text{if} \quad \mathrm{LWP}_{19V} \geq 0.70 \text{ mm} \\ \mathrm{LWP}_{37V} & \text{if} \quad \mathrm{LWP}_{37V} \geq 0.28 \text{ mm} \quad \text{or} \quad \mathrm{WVP} \geq 30 \text{ mm}, \\ \mathrm{LWP}_{85H} & \text{otherwise} \end{cases}$$

$$\mathrm{LWP}_{\mathrm{chan}} = a_0[\ln(290 - \mathrm{TB}_1) - a_1 - a_2\ln(290 - \mathrm{TB}_2)],$$

TABLE 1. The coefficients for LWP algorithms.

$\mathrm{LWP}_{\mathrm{chan}}$	TB_1, TB_2	a_0	a_1[a]	a_2[a]
LWP_{19V}	TV19, TV22	−3.20[b]	2.80	0.42
LWP_{37V}	TV37, TV22	−1.66[c]	2.90	0.35
LWP_{85H}	TH85, TV22	−0.44[c]	−1.60	1.35

[a] Based on global clear sky measurements.

[b] Based on simulated "measurements" calculated from radiative transfer model.

[c] Based on collocated ground-based and satellite measurements for LWP_{37V} and LWP_{85H}.

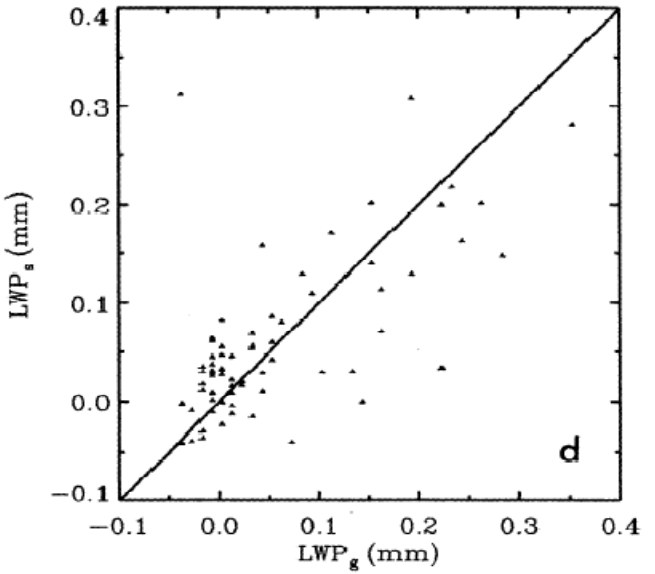

CLOUD LIQUID WATER FROM SSM/I

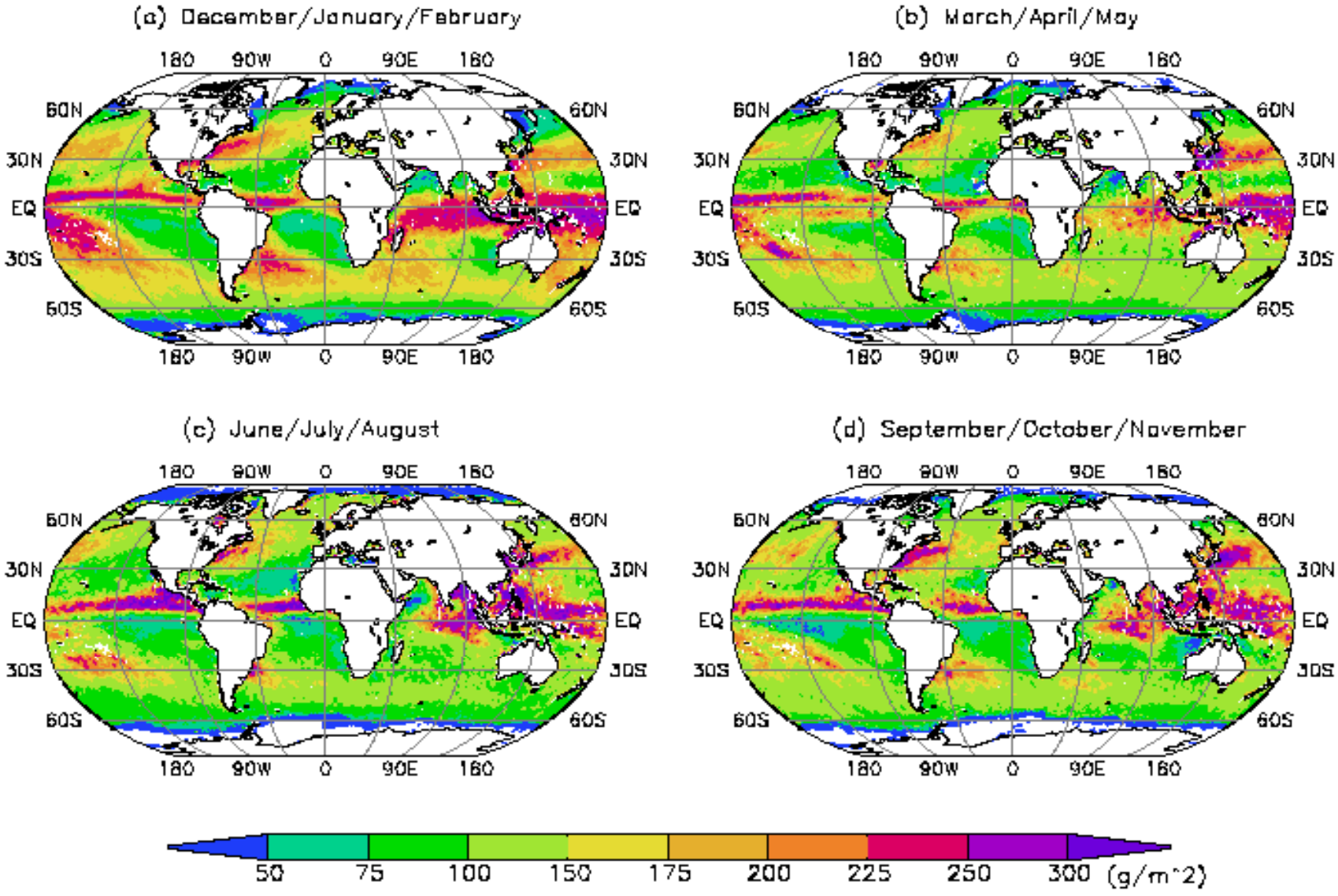

NOAA POES AMSU

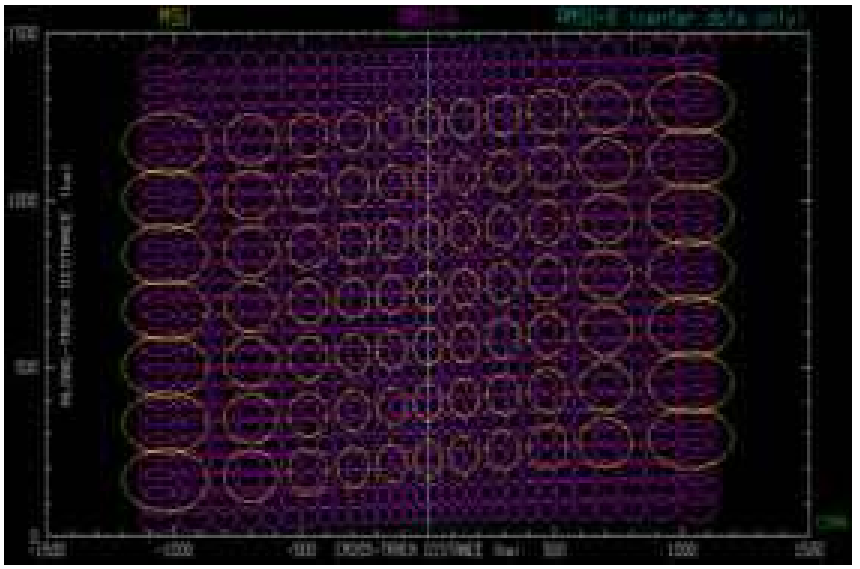

- AMSU are on board NOAA POES since 1998
- There are 20 channels divided into three sub-modules:
  - A1 – 13 channels located near the 60 GHZ oxygen absorption band
  - A2 – 2 window channels at 23.8 and 31.4 GHz
  - B – 2 high frequency channels at 89 and 150 GHz, and 3 channels near 183 GHz water vapor absorption line
- The field-of-view size varies as the instruments scan crossing track

AMSU Weighting Functions

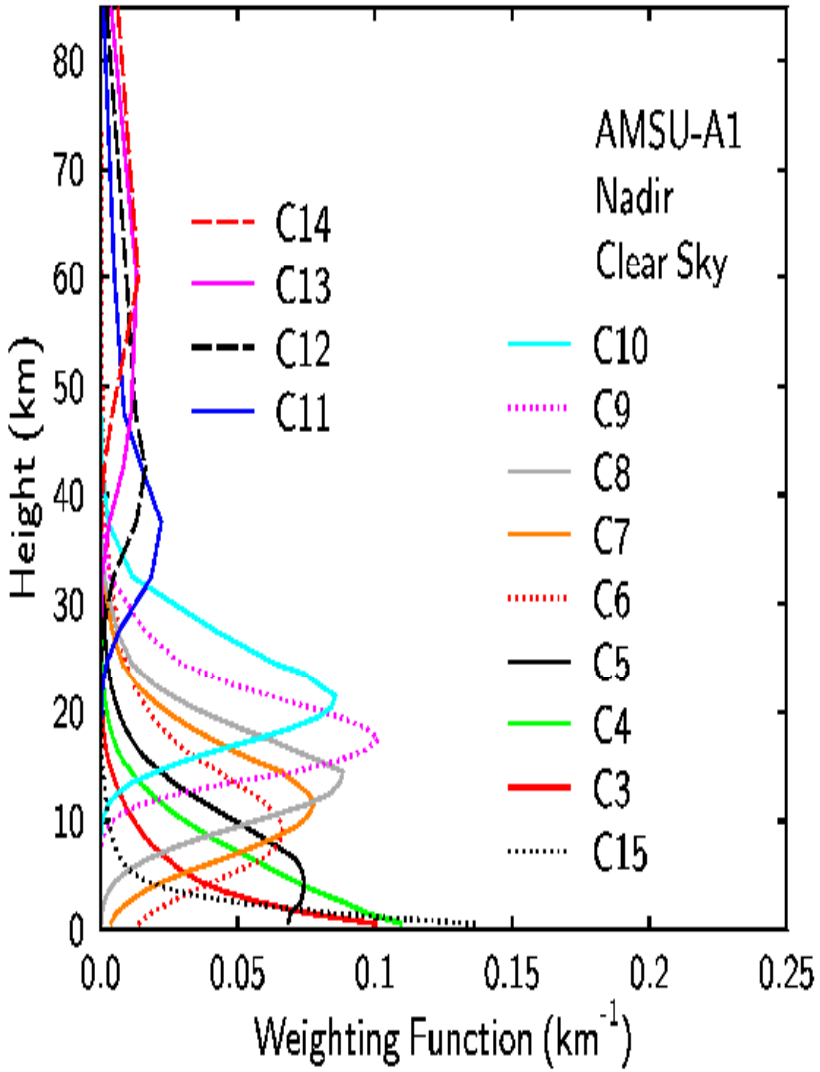

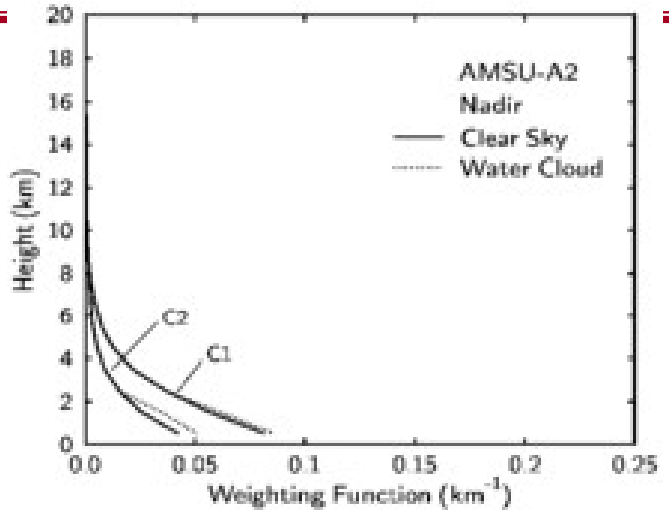

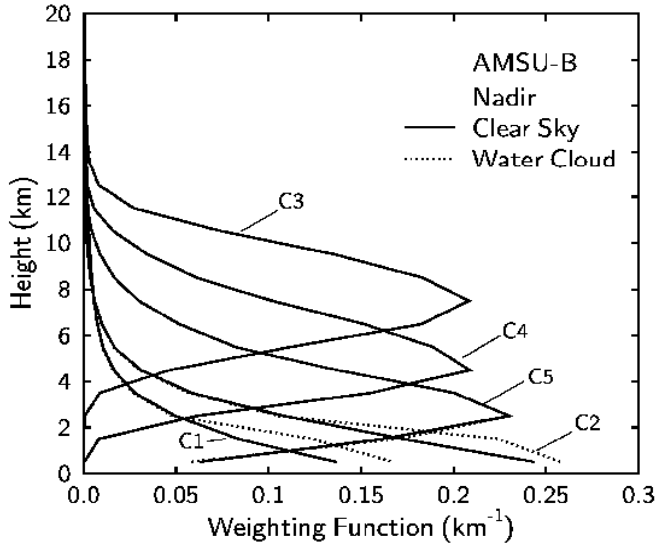

NOAA-16 AMSU-A Radiance Asymmetry (Channel 1,2,3,15)

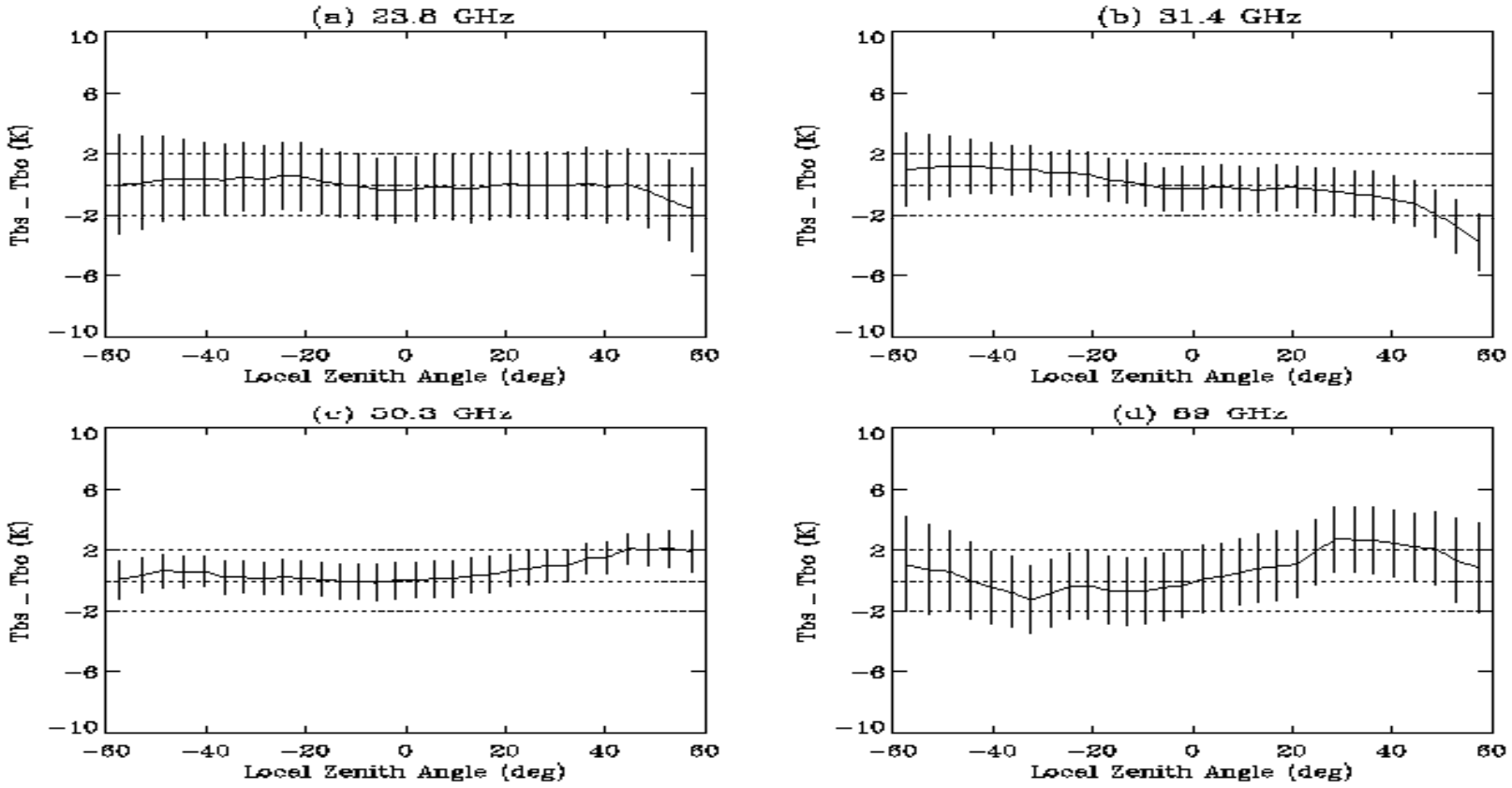

$$\Delta T = A_0 \exp\{ -0.5[(\theta - A_1) / A_2]^2 \} + A_3 + A_4 \theta + A_5 \theta^2$$

NOAA-15 AMSU-A Radiance Asymmetry (Channel 1,2,3,15)

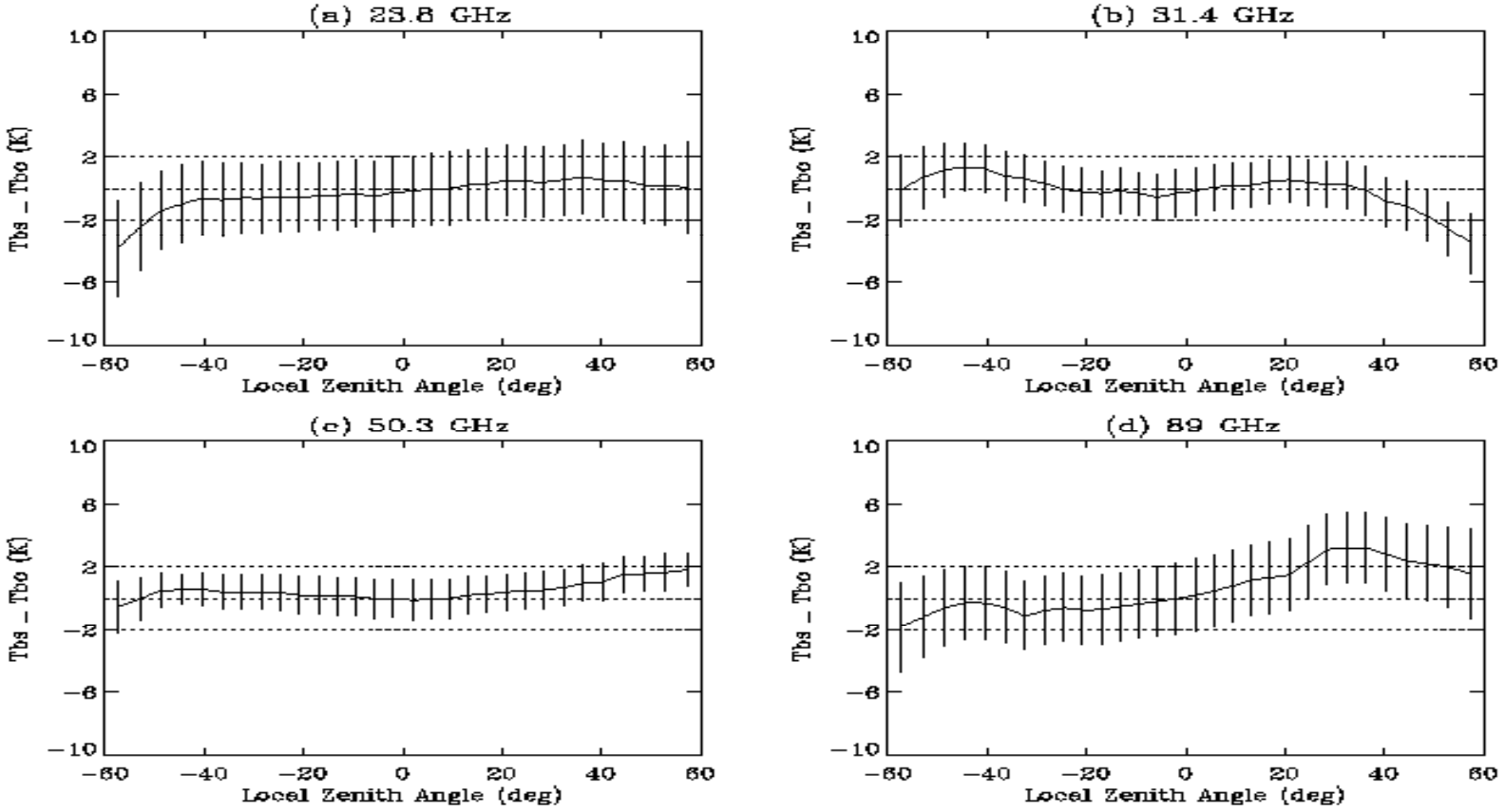

$$\Delta T = A_0 \exp\{ -0.5[(\theta - A_1) / A_2]^2 \} + A_3 + A_4 \theta + A_5 \theta^2$$

Cloud Absorption in relation to Temperature

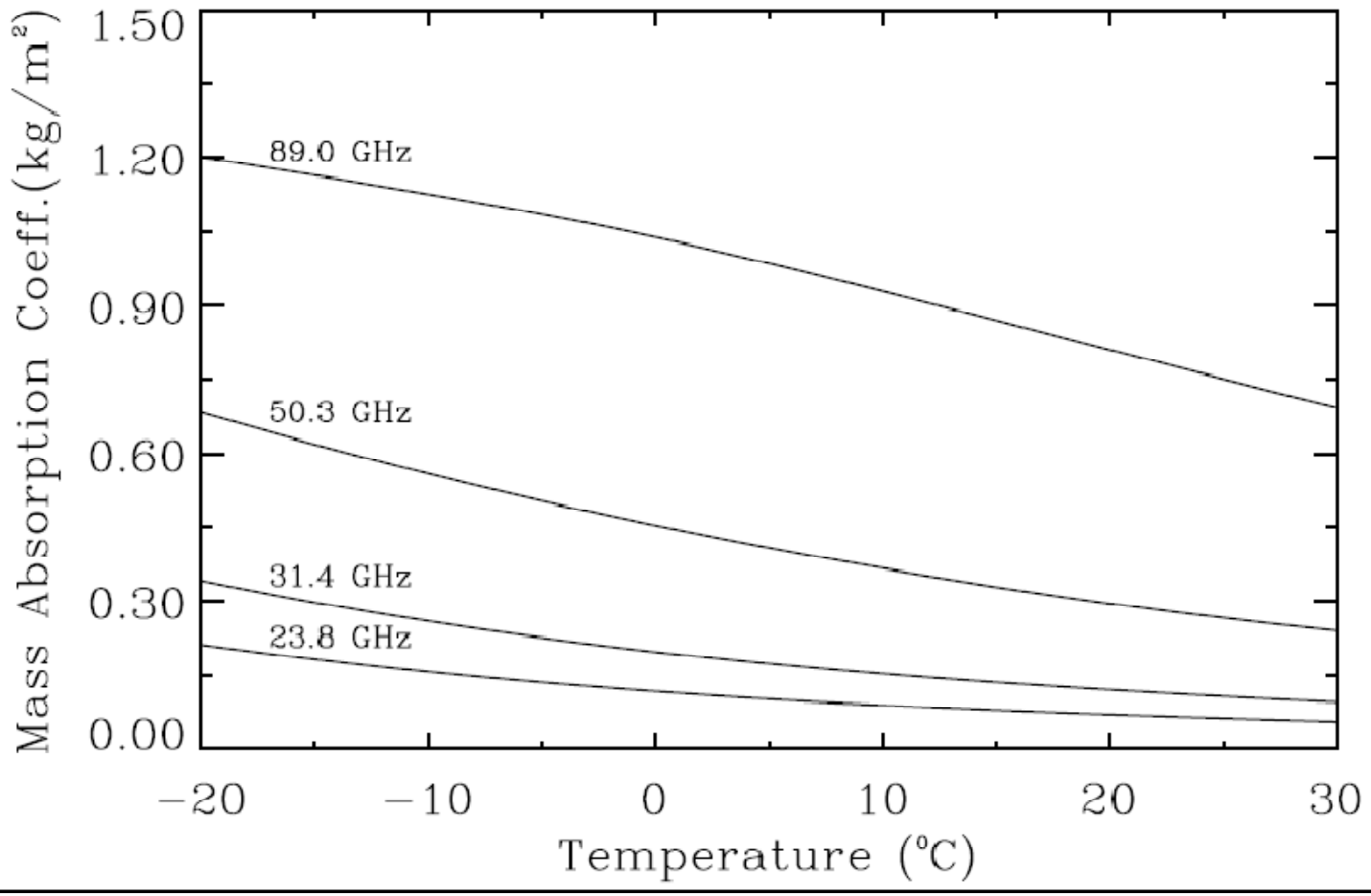

AMSU Cloud Liquid Water

Before Asymmetry Correction

NOAA-15

After Asymmetry Correction

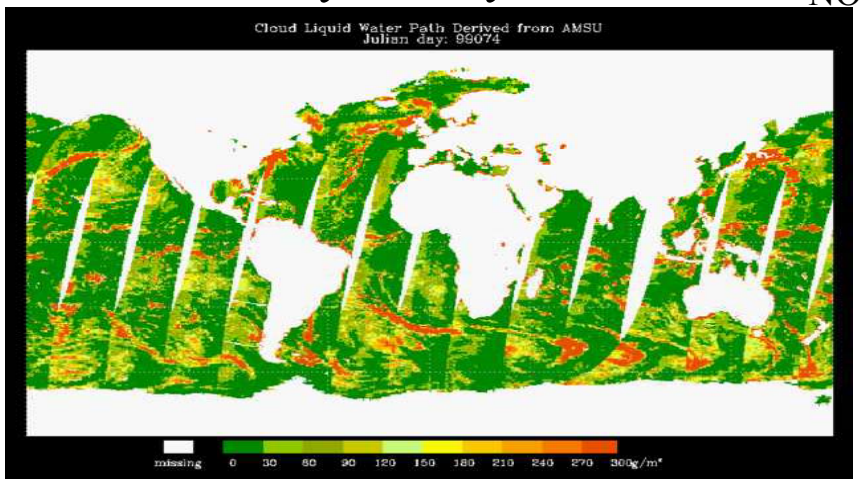

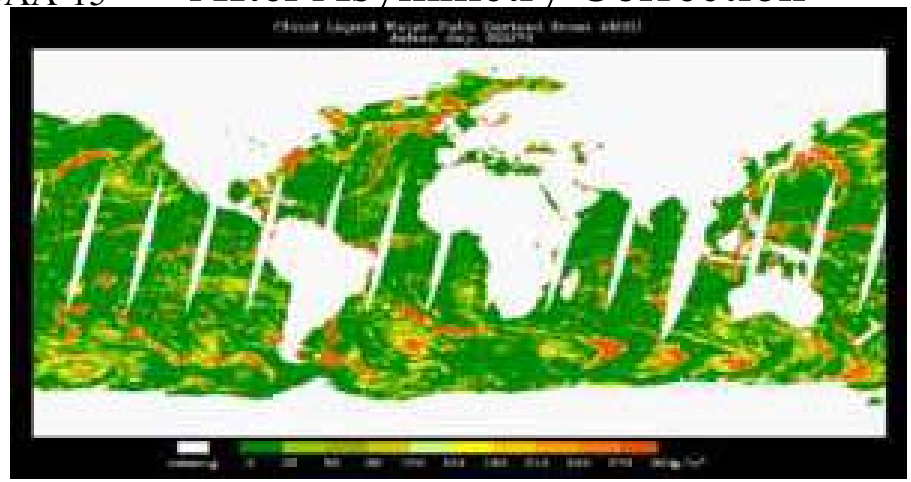

NOAA-16

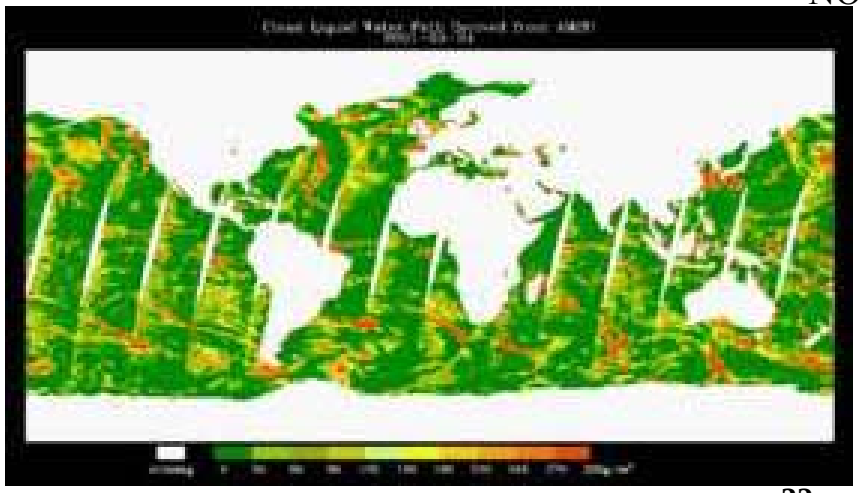

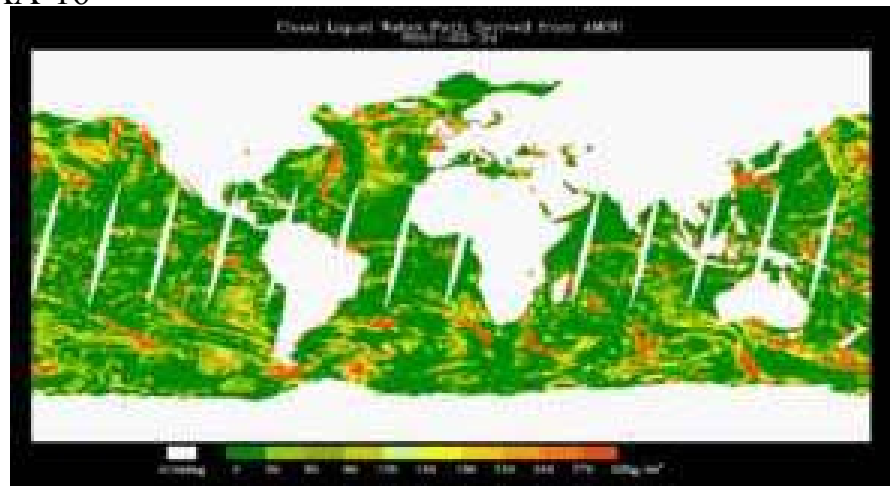

Algorithms of Cloud Ice Water Path: Vertically Integrated Ice Water over Unit Area

Cloud Ice Water Path Algorithm

$$I(\tau,\mu)=\frac{(I_0-B)[\gamma_1 e^{-\kappa(\tau-\tau_1)}-\gamma_2 e^{\kappa(\tau-\tau_1)}]-(I_1-B)[\beta^{-1}e^{\kappa(\tau-\tau_0)}-\beta e^{-\kappa(\tau-\tau_0)}]}{\gamma_4 e^{-\kappa(\tau_1-\tau_0)}-\gamma_3 e^{\kappa(\tau_1-\tau_0)}}+B$$

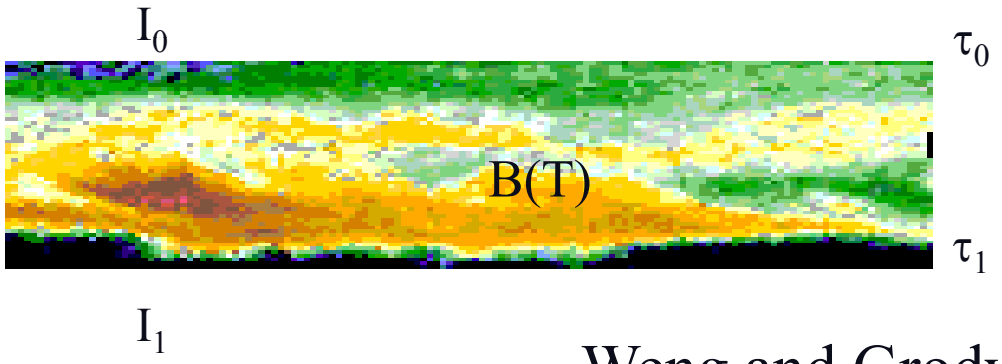

Weng and Grody (2000, JAS)
Zhao and Weng (2002, JAM)

Asymptotic Limits:

1. Emission Approach

$$I(\tau_1,\mu)=B[1-(1-\varepsilon)e^{-2\tau_1/\mu}]-[B(T_s)-B(T)](1-e^{-\tau_1/\mu})[1+(1-\varepsilon)e^{-\tau_1/\mu}]$$

2. Scattering Approach:

$$I(\tau_0,\mu)=\frac{I(\tau_1,\mu)}{1+\Omega(\mu)} \qquad \Omega(\mu)=\frac{IWP}{\mu\rho_i D_e}\Omega_N(x_e,m)$$

Definitions of Cloud Ice Water Path

The influence of cloud microphysical parameters on microwave measurements may be quantitatively analyzed with the model developed in the previous section. The scattering parameter given in Eq. (3) is related to the cloud ice water path and particle size.

The optical thickness is

$$\tau = \int_{z_b}^{z_t} dz \int_0^\infty \frac{\pi}{4} D^2 Q_{\text{ext}}(x, m) N(D)\, dD, \qquad (6)$$

where $N(D)$ is the particle size distribution function, Q_{ext} the extinction efficiency of ice particles, x the particle size parameter, and m the complex refractive index. For ice particles, m is nearly constant at microwave frequencies. The cloud IWP is also related to the particle size distribution by

$$\text{IWP} = \int_{z_b}^{z_t} dz \int_0^\infty \frac{\pi}{6} \rho_i D^3 N(D)\, dD, \qquad (7)$$

where ρ_i is the particle bulk density.

A monodispersed (uniform) type of $N(D)$ is considered first so that the scattering parameter can be directly related to the cloud microphysical parameters. For a cloud having a thickness, δz, the optical thickness is

$$\tau = \delta z N_t \frac{\pi D^2}{4} Q_{\text{ext}}(x, m) \quad \text{and} \qquad (8)$$

$$\text{IWP} = \delta z \frac{\pi}{6} \rho_i N_t D^3. \qquad (9)$$

Thus τ can be expressed in terms of the IWP and the extinction cross section, namely,

$$\tau = \frac{3}{2} \frac{\text{IWP}}{\rho_i D} Q_{\text{ext}}(x, m), \qquad (10)$$

and Ω is obtained by substituting Eq. (10) into Eq. (3):

$$\Omega(\mu) = \frac{\text{IWP}}{\mu \rho_i D} \Omega_N(x, m), \qquad (11)$$

where $x = (\pi D)/\lambda$ and Ω_N is the normalized scattering parameter, which is given by

$$\Omega_N(x, m) = \frac{3}{4}[Q_{\text{ext}}(x, m) - Q_{\text{sca}}(x, m) g(x, m)]. \qquad (12)$$

From Eq. (11), it is evident that the large scattering parameter is directly proportional to the IWP. However, the relationship between Ω and D is nonlinear due to Ω_N and may also depend on the particular particle size distribution.

For polydispersed particles, Ω is calculated using Eq. (3). The optical parameters are derived through integrating over the entire range of particle diameters for a given size distribution. Using a gamma function that has an exponent of 2 (Ulbrich 1983) for the polydispersed particles, Ω is given as

$$\Omega(\mu) = \frac{\text{IWP}}{\mu \rho_i D_e} \Omega_N(x_e, m), \qquad (13)$$

where $x_e = (\pi D_e)/\lambda$ and D_e is the particle effective diameter, which is defined as

$$D_e = \frac{\int_0^\infty N(D) D^3\, dD}{\int_0^\infty N(D) D^2\, dD}. \qquad (14)$$

CIWP Error Budget

$$\Omega(\mu) = \frac{IWP}{\mu \rho_i D_e} \Omega_N(x_e, m)$$

The errors of CIWP are mainly due to

(1) uncertainty in the effective particle diameters

(2) uncertainty in the particle bulk volume density

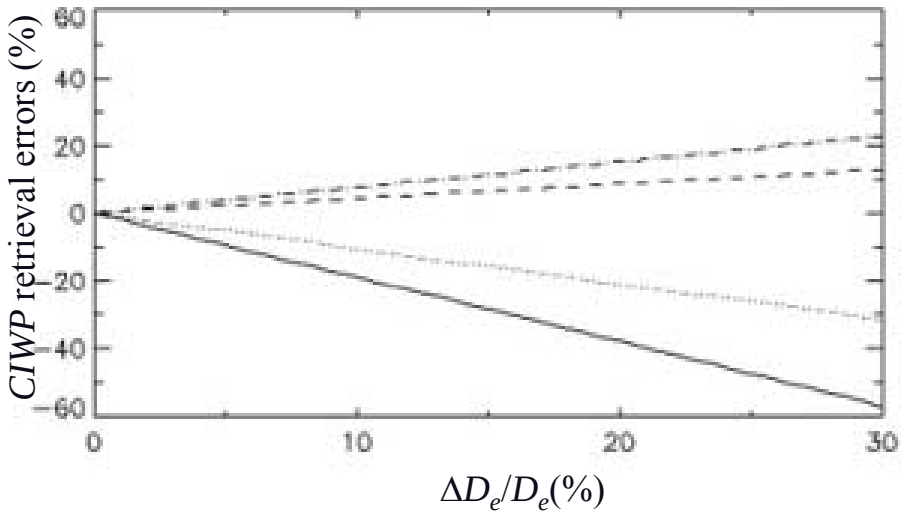

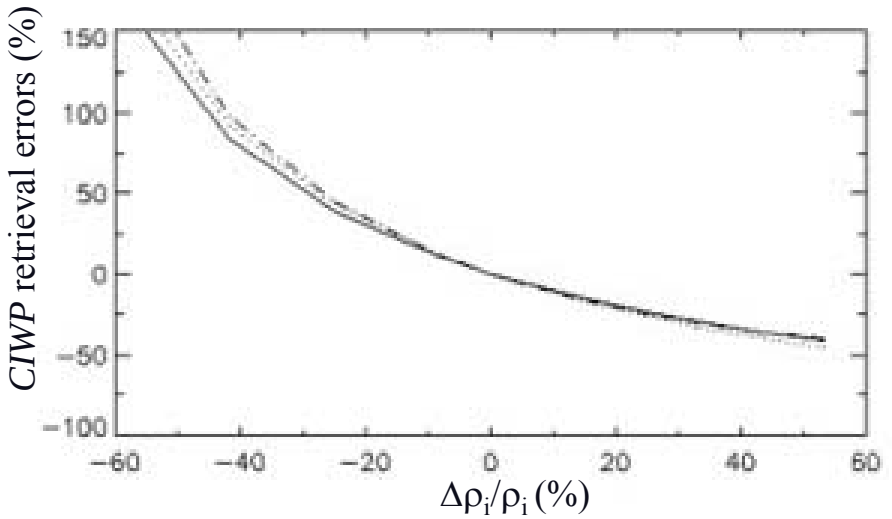

ER-2 MIR, DC-8 ARMAR, MODIS Simulator Measurements

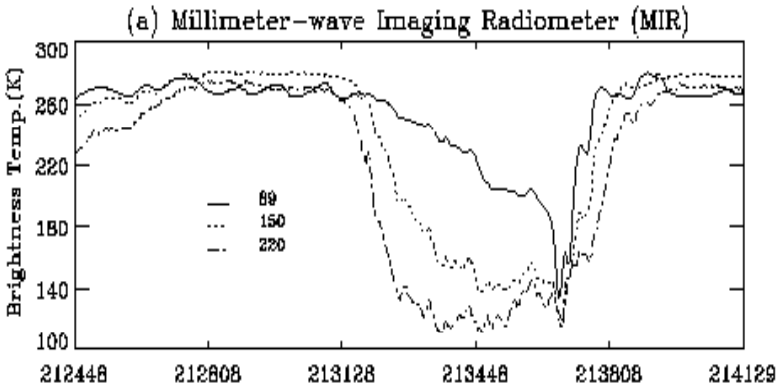

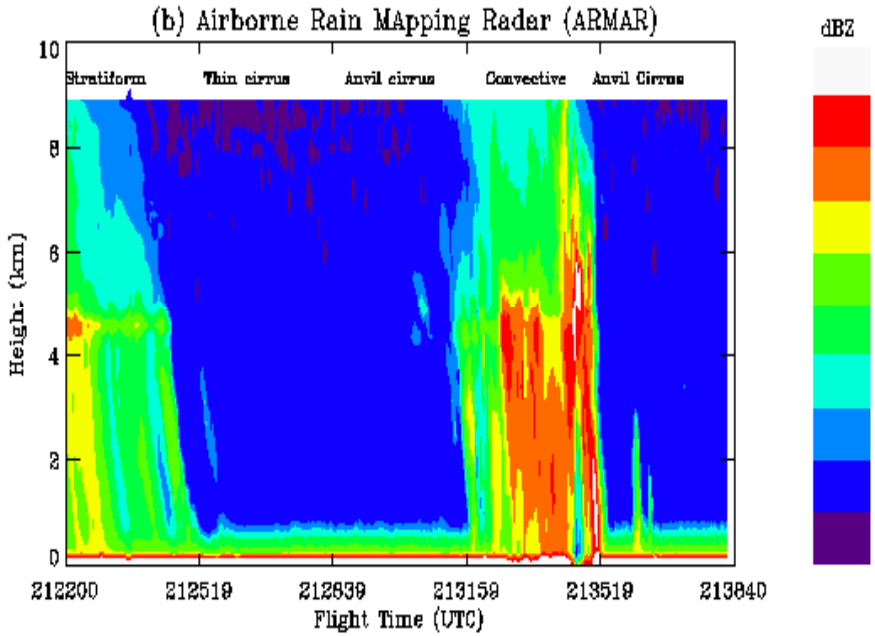

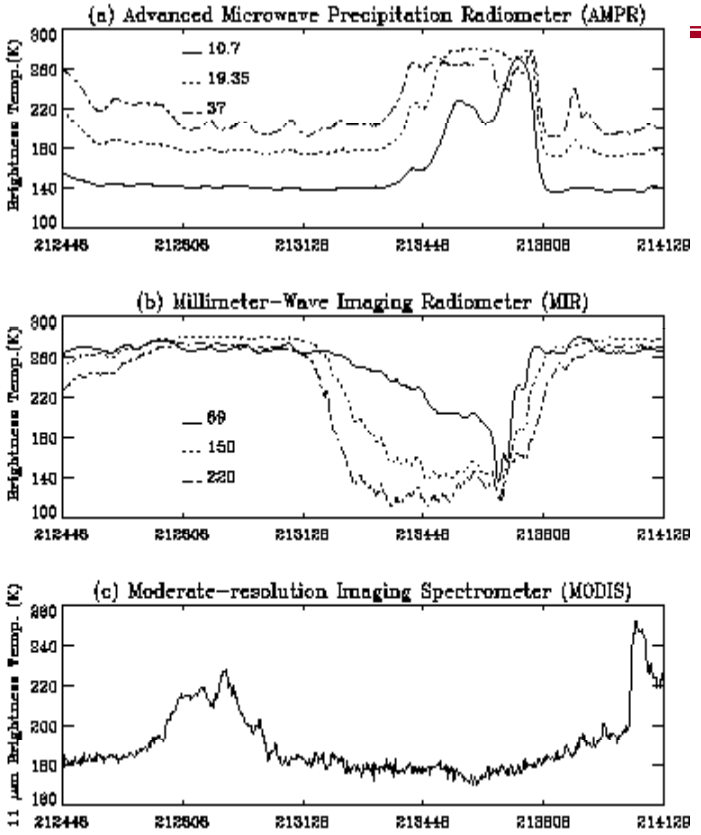

Three millimeter wavelength channels provide the overa needed sensitivity for cloud ice microphysics which can be uniquely used for precipitation mapping

Weng and Grody (2000, JAS)

MIR Window & Sounding Channel Observations

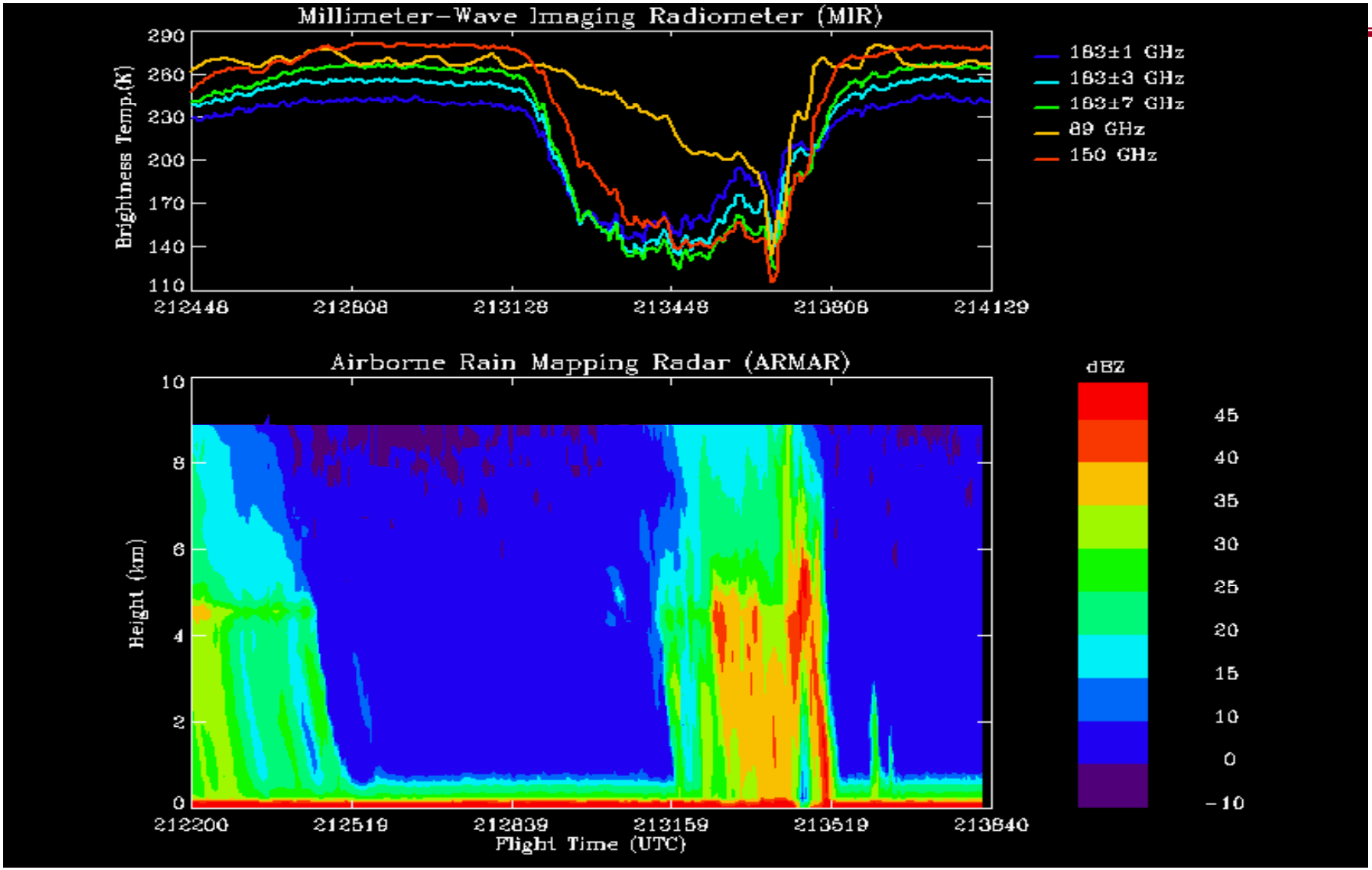

Flowchart of Cloud Ice Algorithm

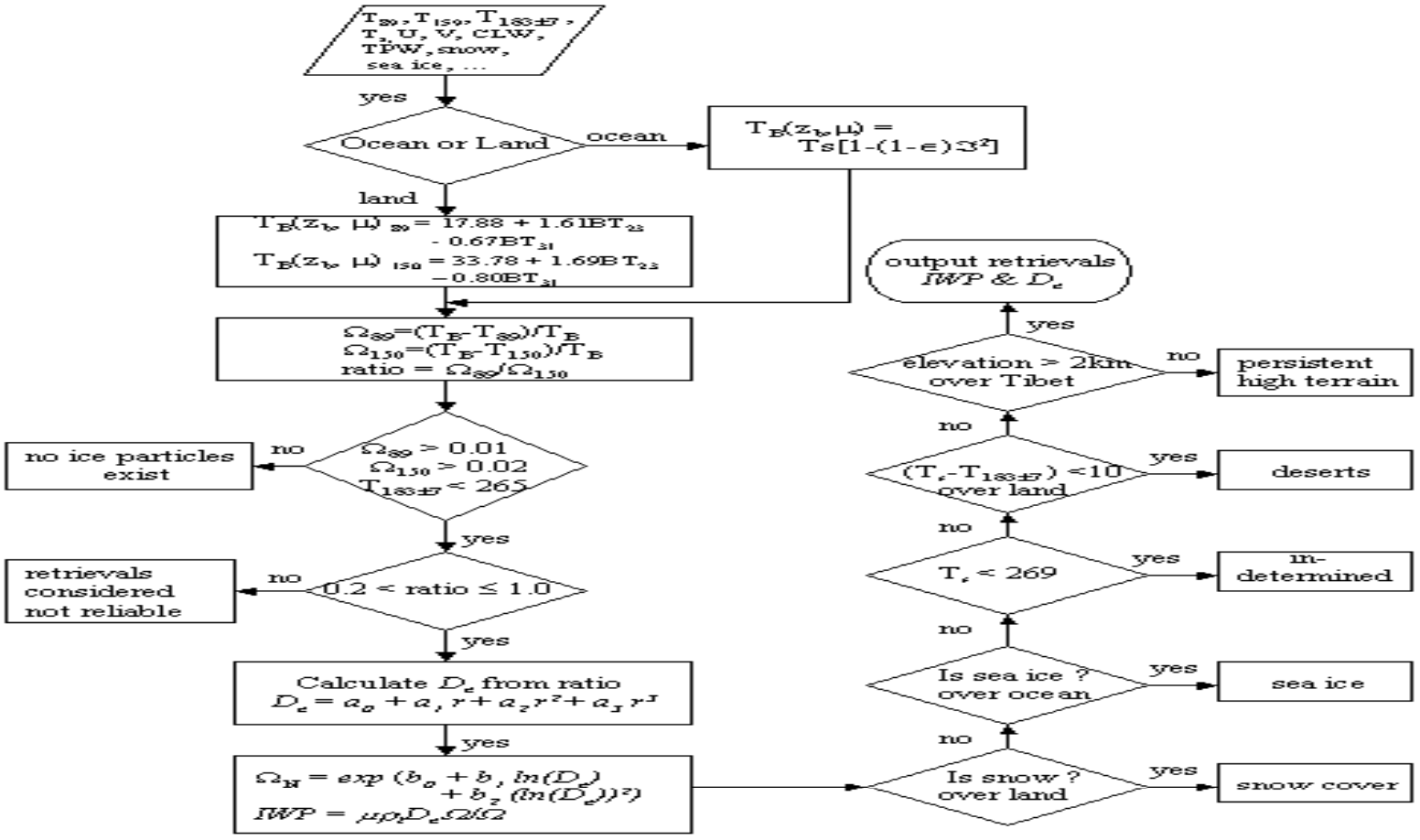

The flow chart of the global *IWP* and D_e retrieval algorithm

Cloud Ice Water Path

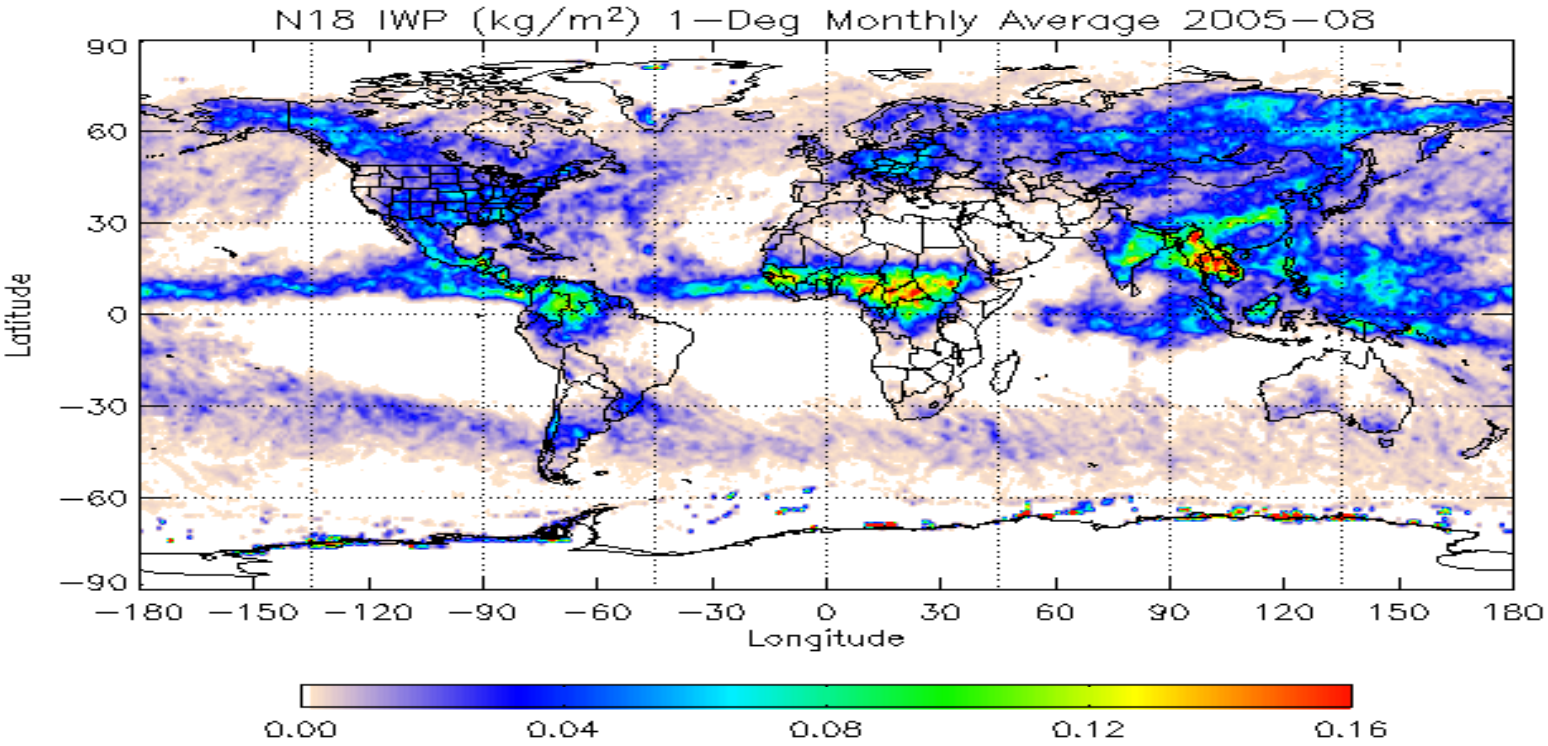

- **Brightness temperatures from AMSU-B 89 and 150 GHz are two primary channels for IWP and De**
- **Retrieval algorithm was published in Journal of Atmos Sci (Weng and Gody, 2000) and J. Appli. Meteor (Zhao and Weng, 2002)**
- **AMSU-A window channels are used for surface screening.**
- **The algorithm works for opaque ice clouds having IWP greater than 0.05 kg/m2**

Algorithms of Atmospheric Sounding

National Environmental Satellite, Data, and Information Service

MIRS System Design & Architecture

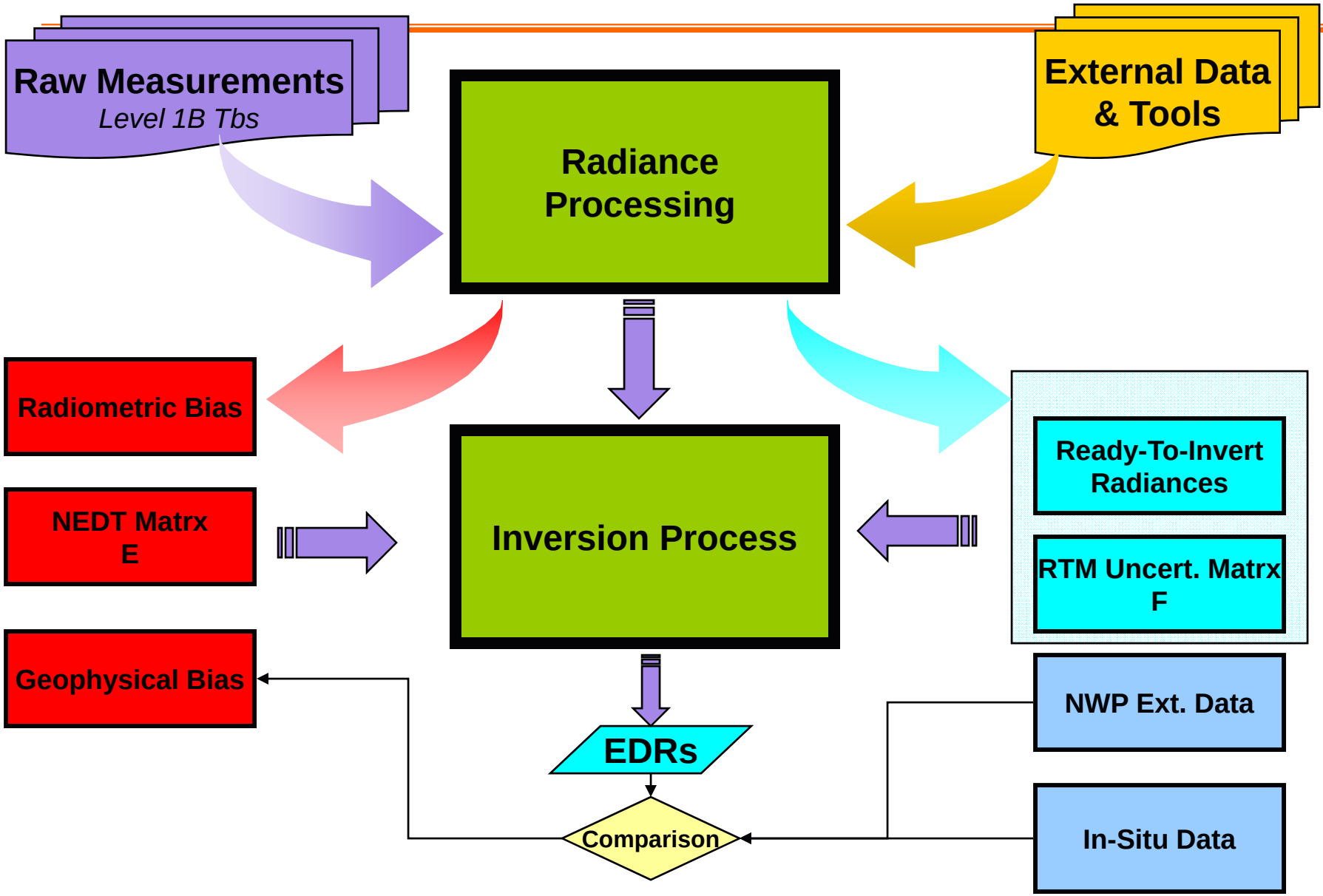

National Environmental Satellite, Data, and Information Service

Cost Function Minimization

- To find the optimal solution, solve for:

$$J(X) = \left[\frac{1}{2}(X - X_0)^T \times E^{-1} \times (X - X_0)\right] + \left[\frac{1}{2}(Y'' - Y(X))^T \times E^{-1} \times (Y'' - Y(X))\right]$$

- Assuming linearity

$$\frac{\partial J(X)}{\partial X} = J'(X) = 0$$

- This leads to two iterative solution:

$$y(x) = y(x_0) + K[x - x_0]$$

  - when number of parameters << channel

$$\Delta X_{n+1} = \left\{\left(B^{-1} + K_n^T E^{-1} K_n\right)^{-1} K_n^T E^{-1}\right\}\left[\left(Y^m - Y(X_n)\right) + K_n \Delta X_n\right]$$

  - Otherwise

$$\Delta X_{n+1} = \left\{BK_n^T\left(K_n BK_n^T + E\right)^{-1}\right\}\left[\left(Y^m - Y(X_n)\right) + K_n \Delta X_n\right]$$

National Environmental Satellite, Data, and Information Service

Microwave TPW Extended over Land

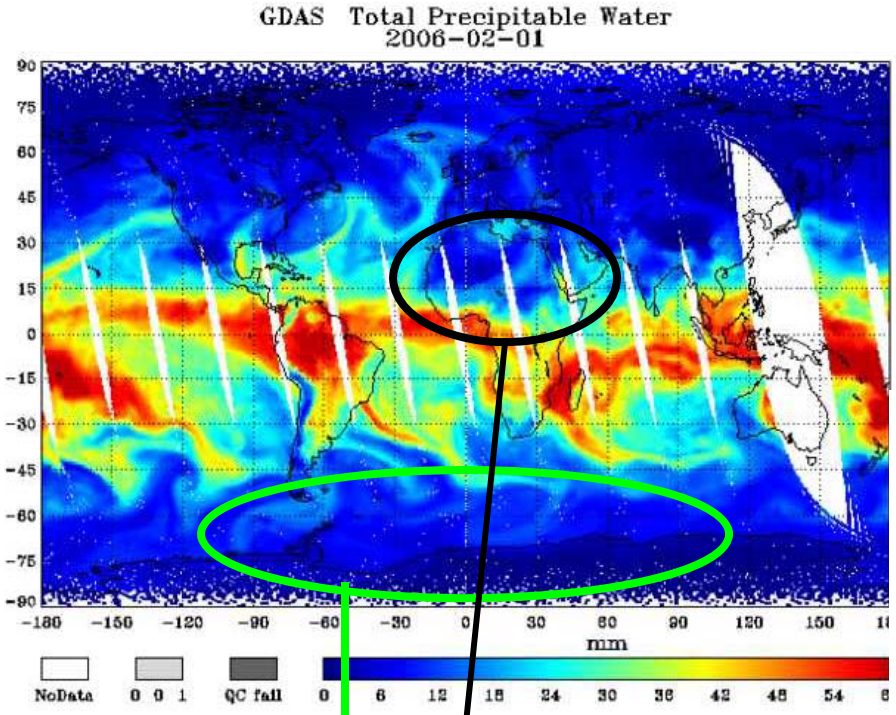

GDAS Analysis

snow-covered surfaces need better handling

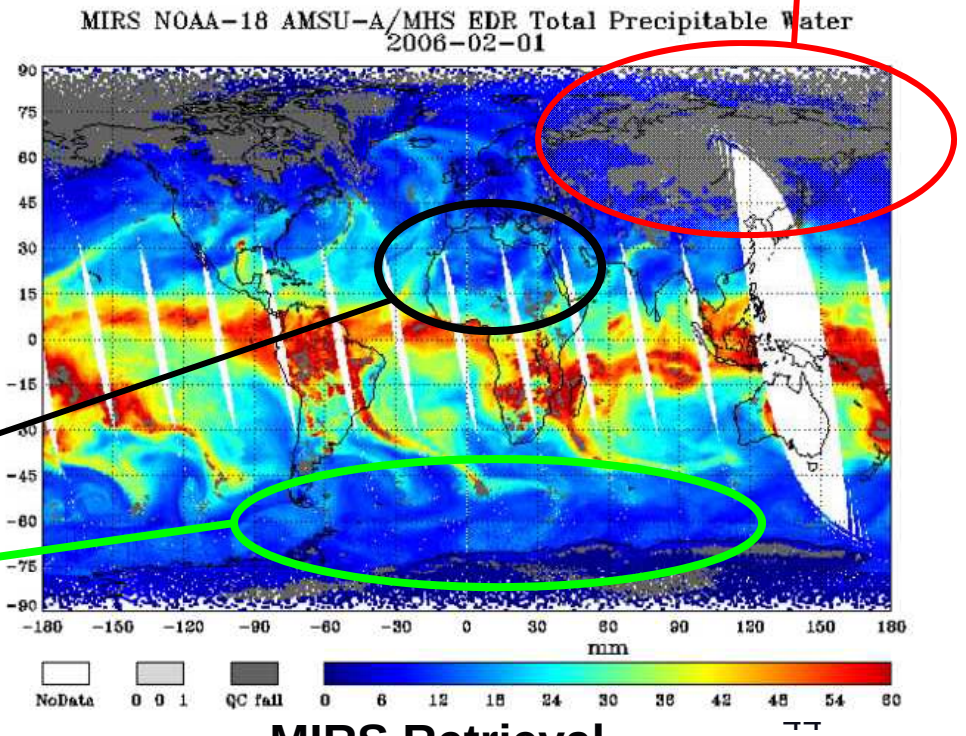

MIRS Retrieval

Retrieval over sea-ice and most land areas capturing same features as GDAS

Validation of TPW Retrieval over Land

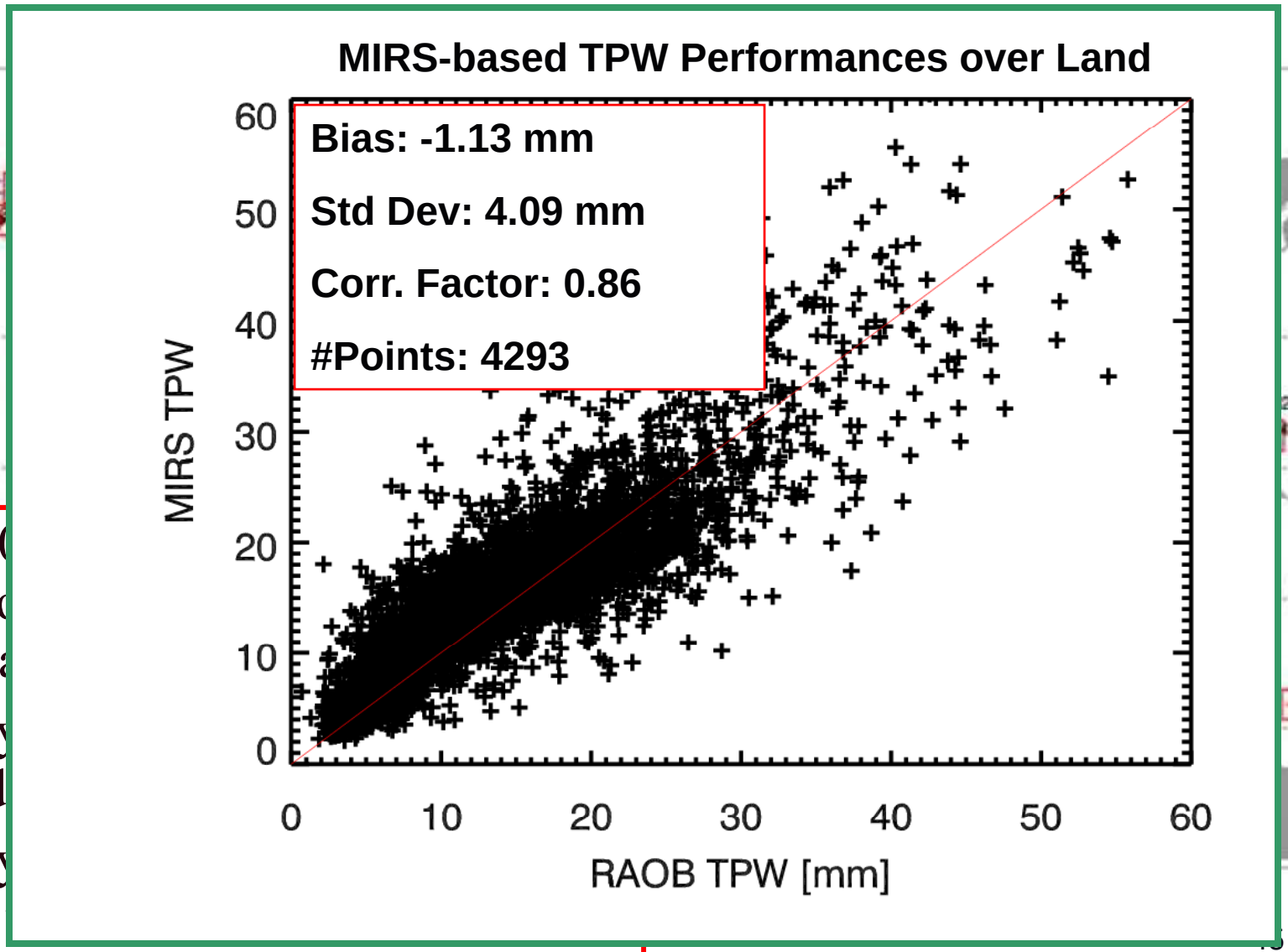

- ~400 collo radia
- Only land
- Only and
- Cloudy points included, up to

National Environmental Satellite, Data, and Information Service

Global Temperature Profiling

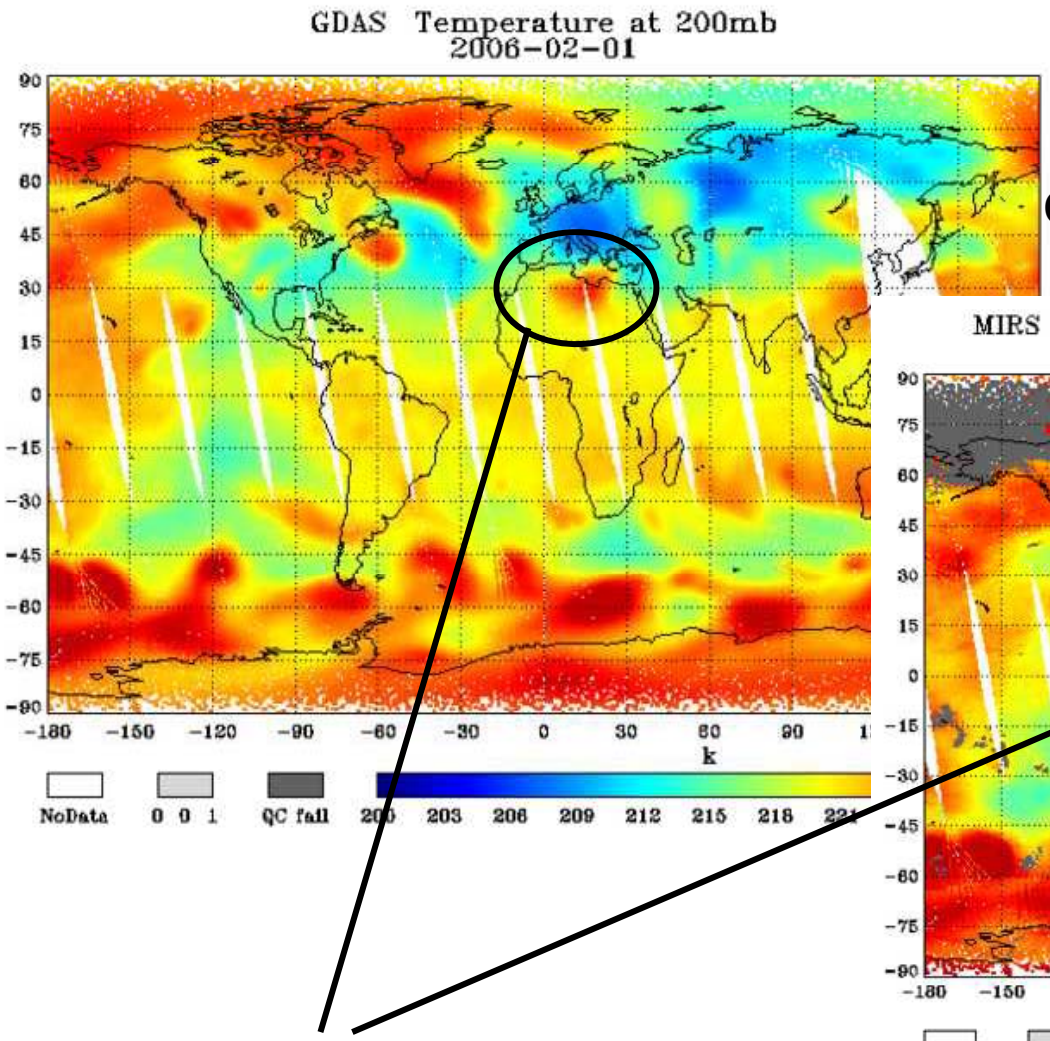

No Scan-Dependence in retrieval
Smooth Transition Land/Ocean

QC-failure is based on convergence:
Focus of on-going work

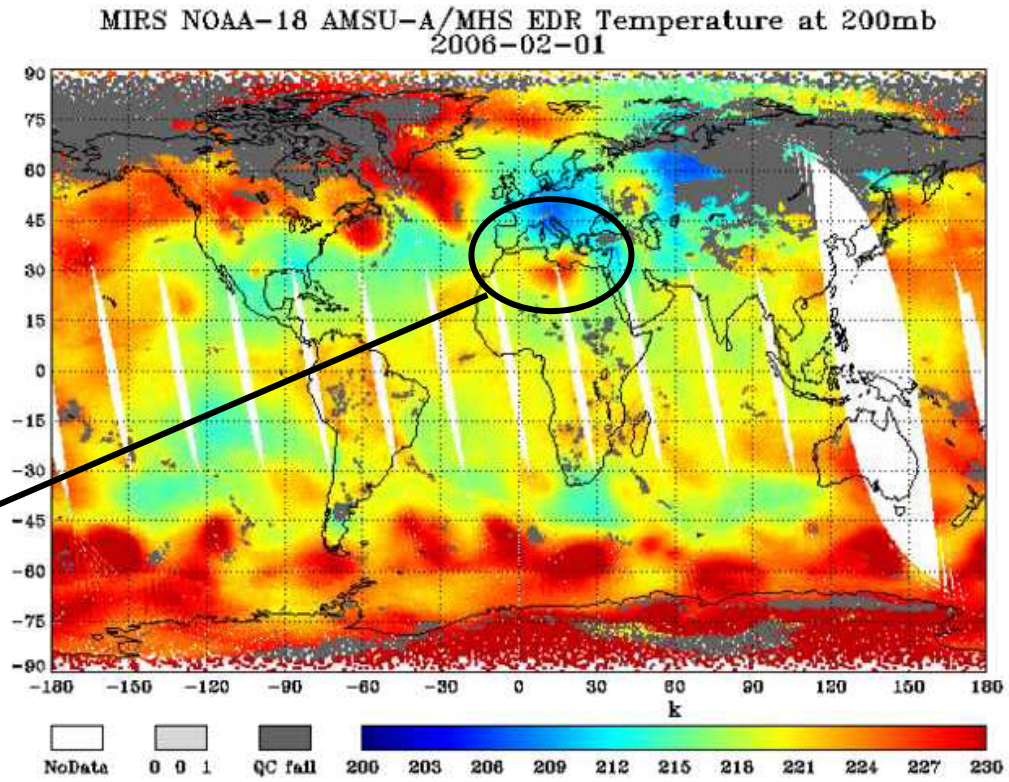

Similar Features Captured

National Environmental Satellite, Data, and Information Service

Global Humidity Profiling

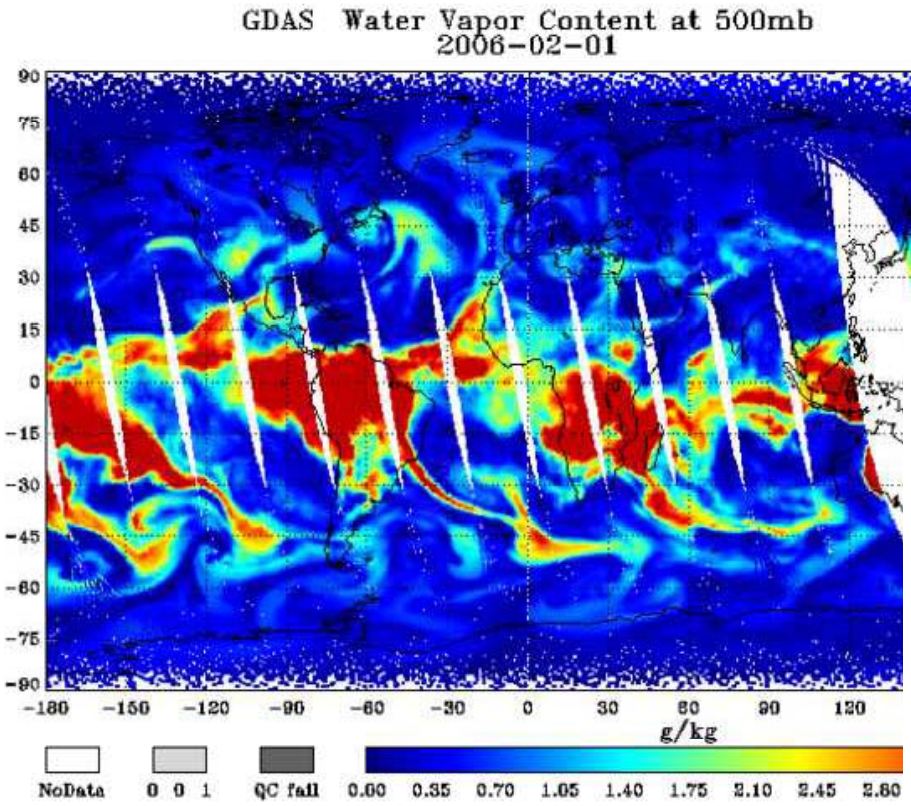

No Scan-dependence noticed: Angle dependence properly accounted for

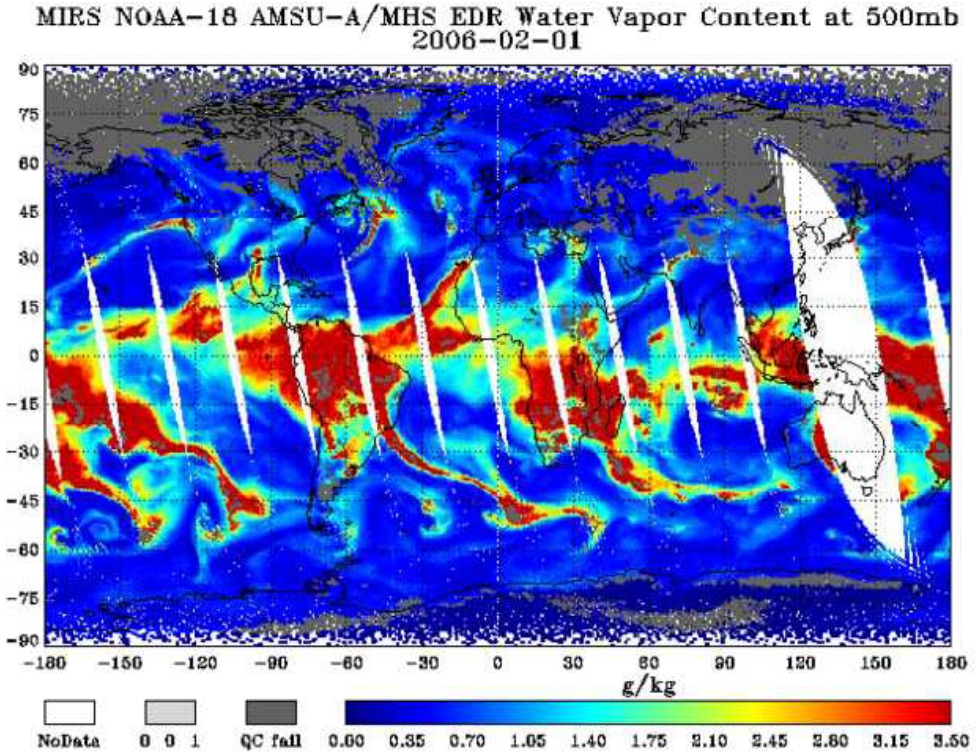

Outline

- **Microwave Remote Sensing Theory**
  - MW gas spectrum
  - Radiative Transfer Approximation
- **Microwave Algorithms**
  - Cloud liquid water
  - Cloud ice water
  - Precipitation
  - Temperature and water vapor
- **Product Applications**
  - Model validation and intercomparison
  - NWP model validations
  - Climate monitoring and trending

National Environmental Satellite, Data, and Information Service

Microwave Environmental Data Records

SDR/EDR	POES/METOP AMSU-A/B; MHS	DMSP SSMIS	NPOESS ATMS/MIS
Radiances	✓	✓	✓
Temp. profile	✓	✓	✓
Moist. profile	✓	✓	✓
Total precipitable water*	✓	✓	✓
Hydr. profile	✓	✓	✓
Precip rate*	✓	✓	✓
Snow cover*	✓	✓	✓
Snow water equivalent*	✓	✓	✓
Sea ice *	✓	✓	✓
Cloud water*	✓	✓	✓
Ice water*	✓	✓	✓
Land temp*	✓	✓	✓
Land emis*	✓	✓	✓
Soil moisture/Wetness Index		✓	✓

Intercomparison between MODIS and AMSR-E LWP for Stratus Clouds

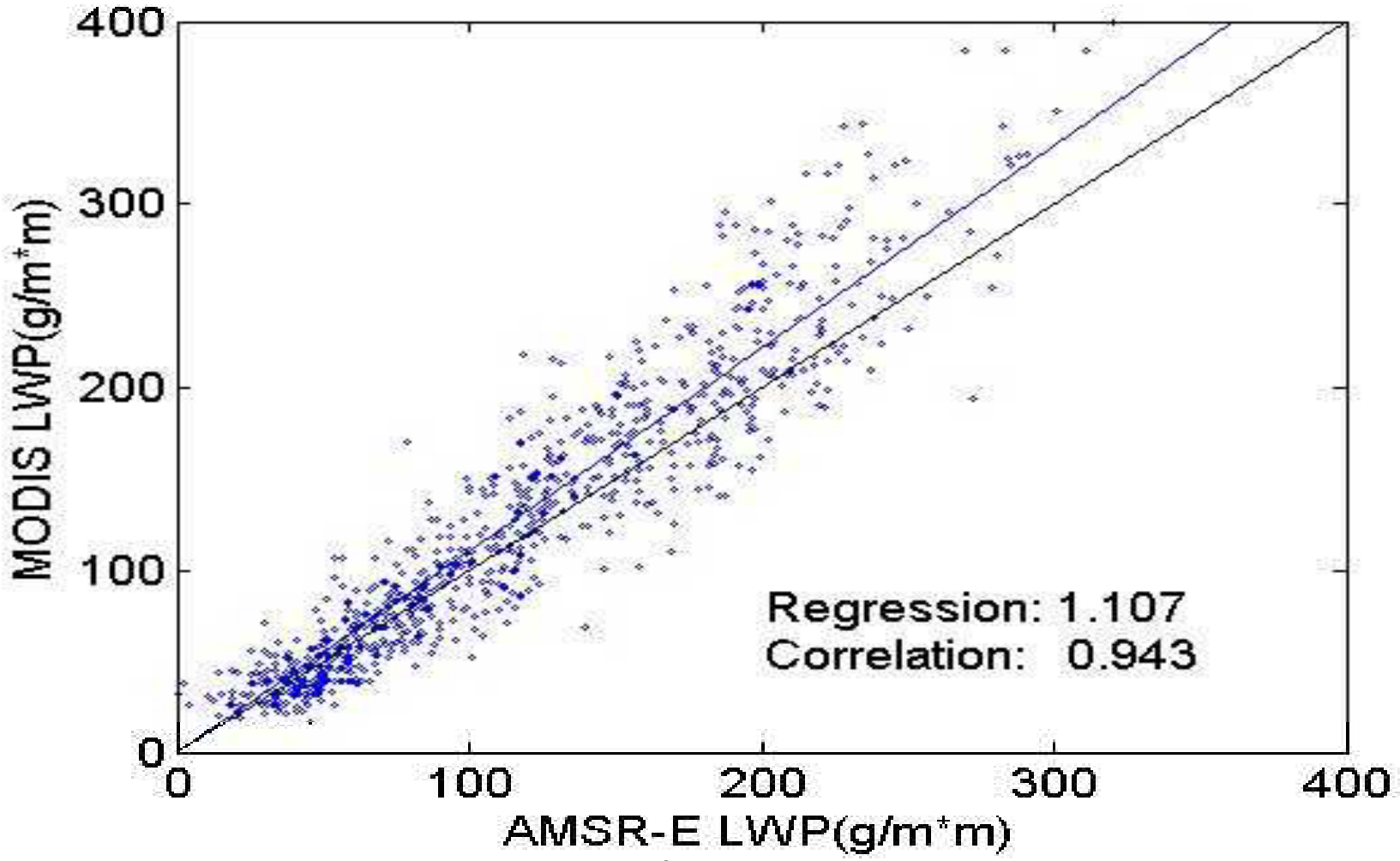

Validation of General Circulation Model

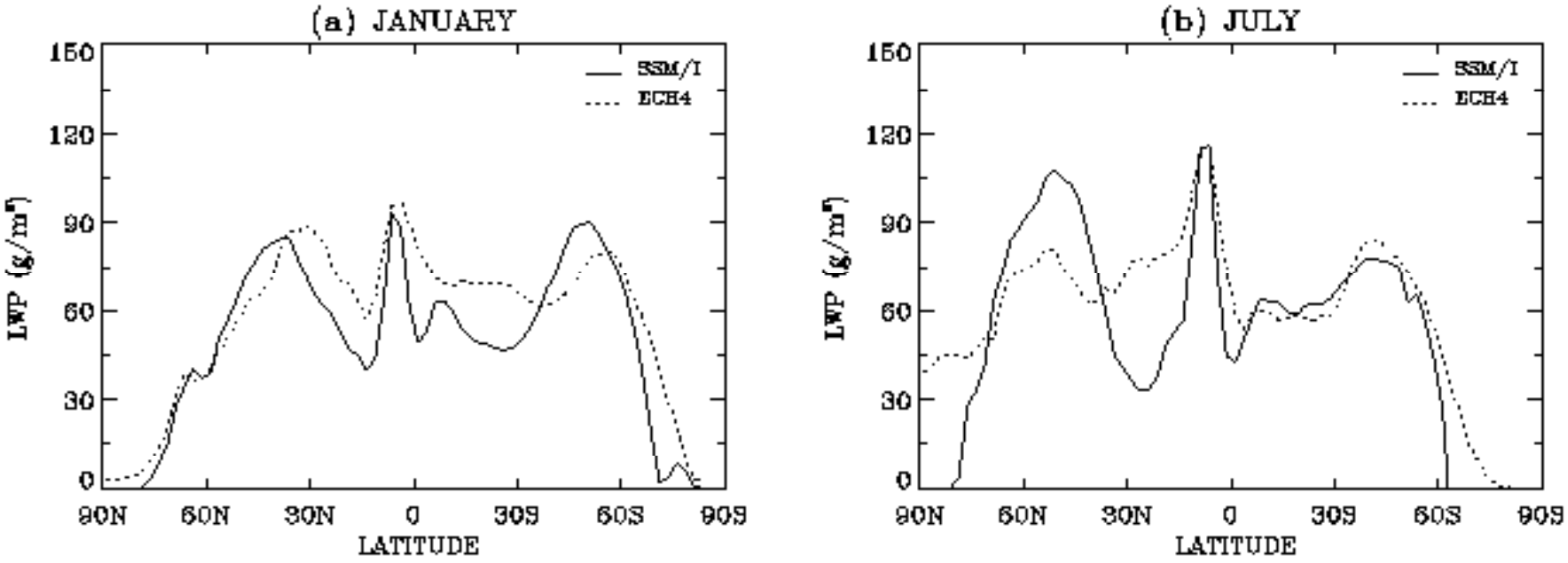

Validation of Numerical Weather Prediction Models

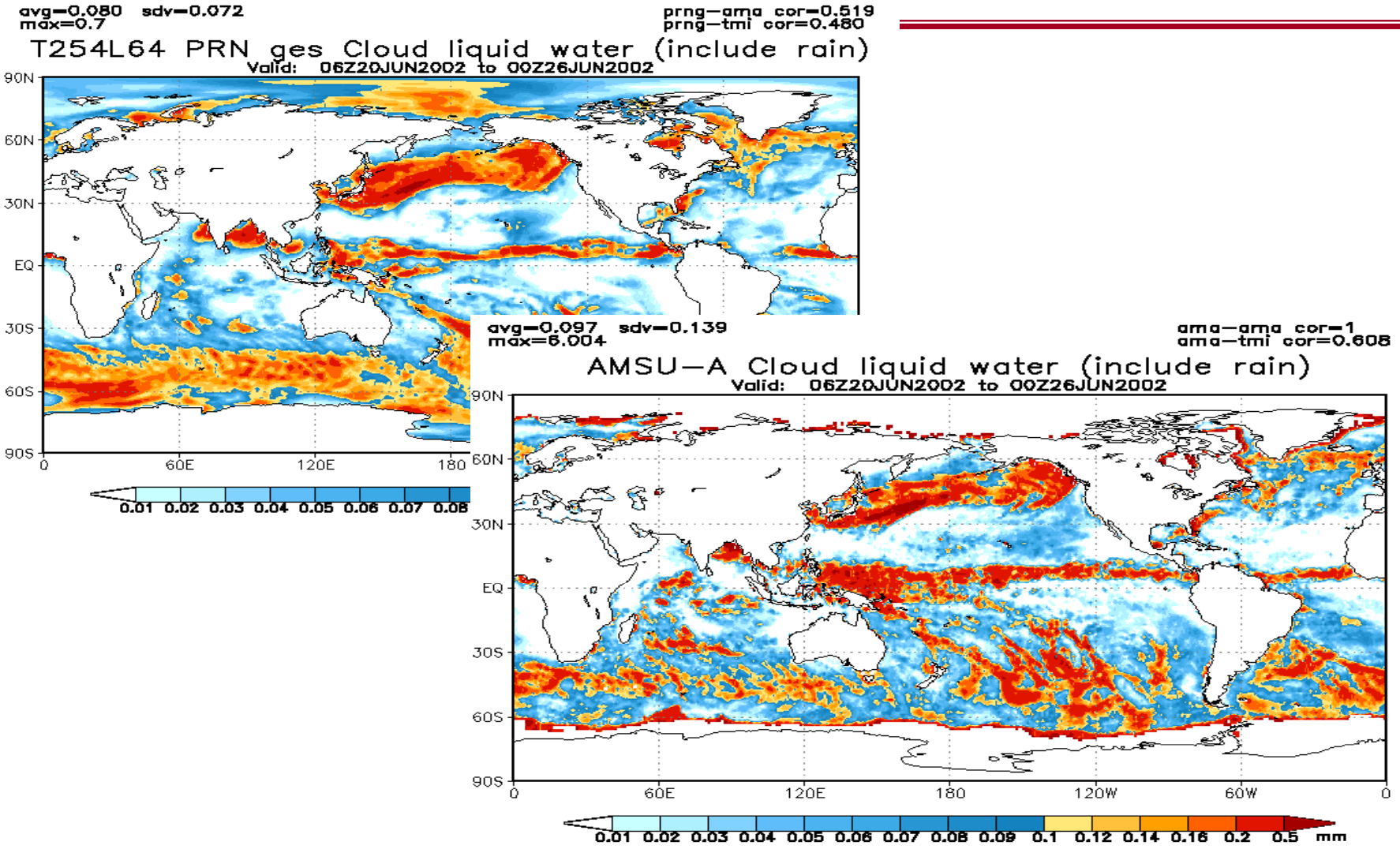

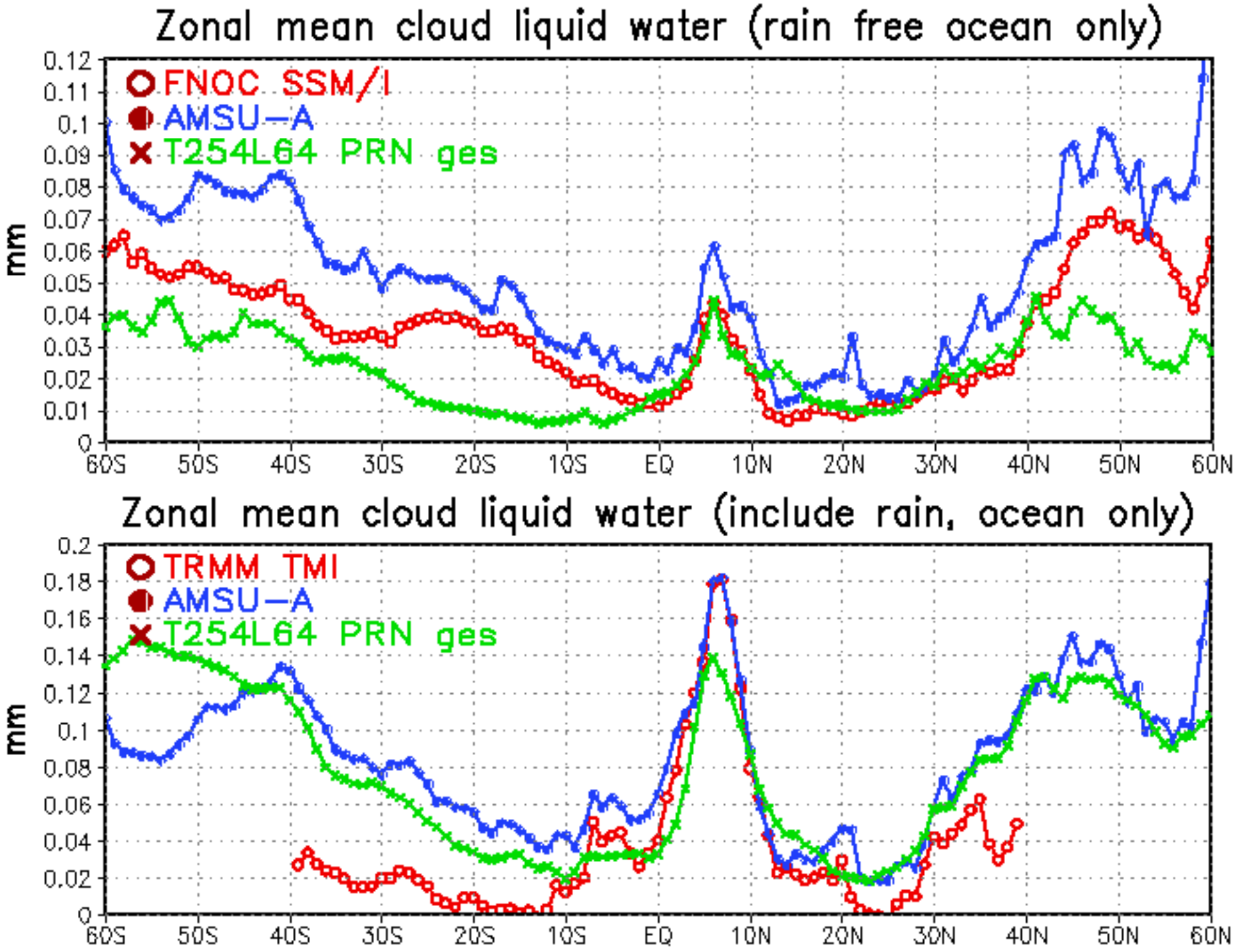
Zonal mean cloud liquid water (rain free ocean only)
FNOC SSM/I
AMSU-A
T254L64 PRN ges
mm
0.12
0.11
0.1
0.09
0.08
0.07
0.06
0.05
0.04
0.03
0.02
0.01
0
60S
50S
40S
30S
20S
10S
EQ
10N
20N
30N
40N
50N
60N
Zonal mean cloud liquid water (include rain, ocean only)
TRMM TMI
AMSU-A
T254L64 PRN ges
mm
0.2
0.18
0.16
0.14
0.12
0.1
0.08
0.06
0.04
0.02
0
60S
50S
40S
30S
20S
10S
EQ
10N
20N
30N
40N
50N
60N

GFS Prognostic Scheme vs. AMSU Cloud Water

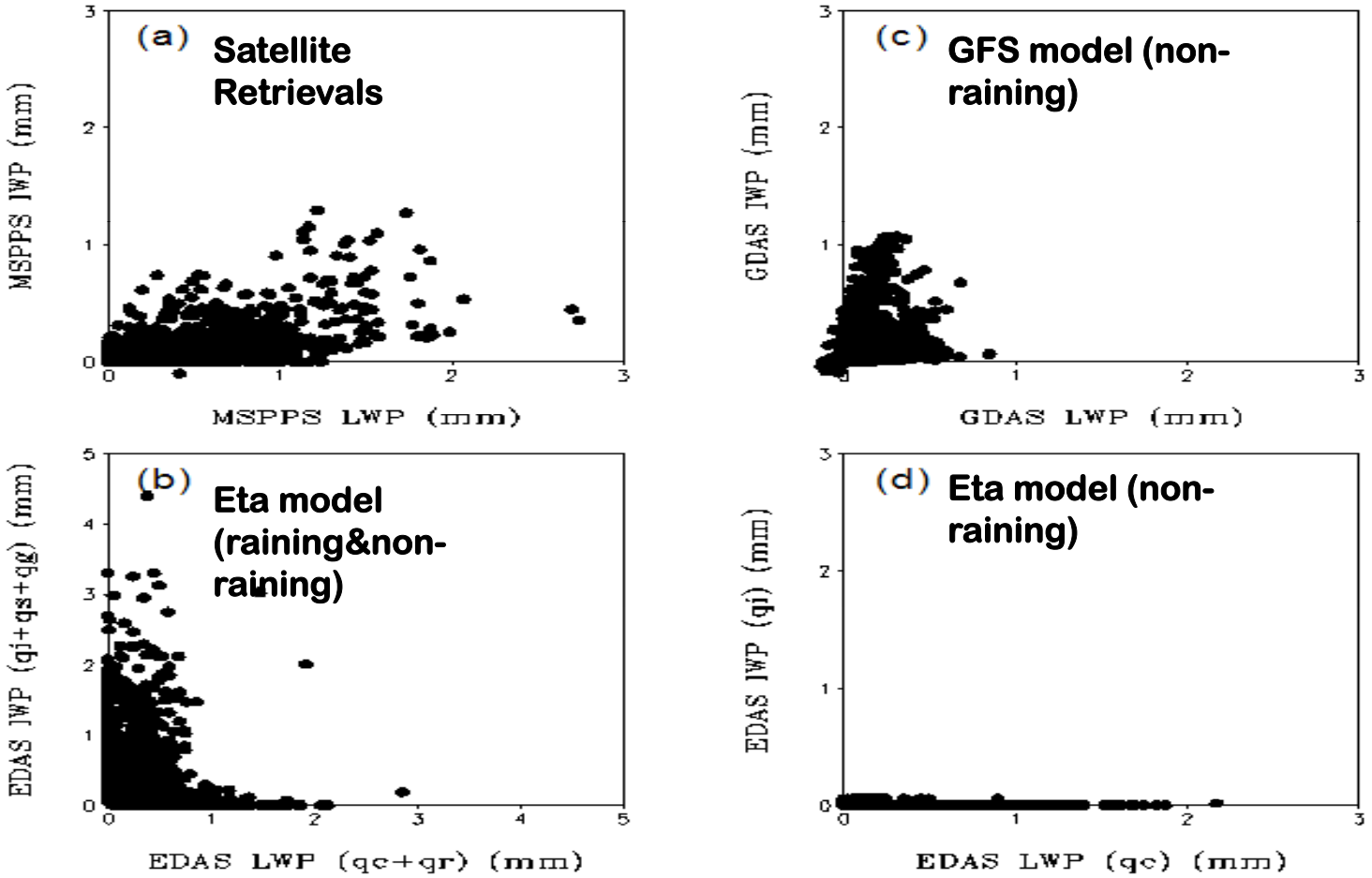

It is obvious that global/regional models have "ice happy" physics

National Environmental Satellite, Data, and Information Service

Impacts of SSMIS LAS on Hurricane Temperature Analysis

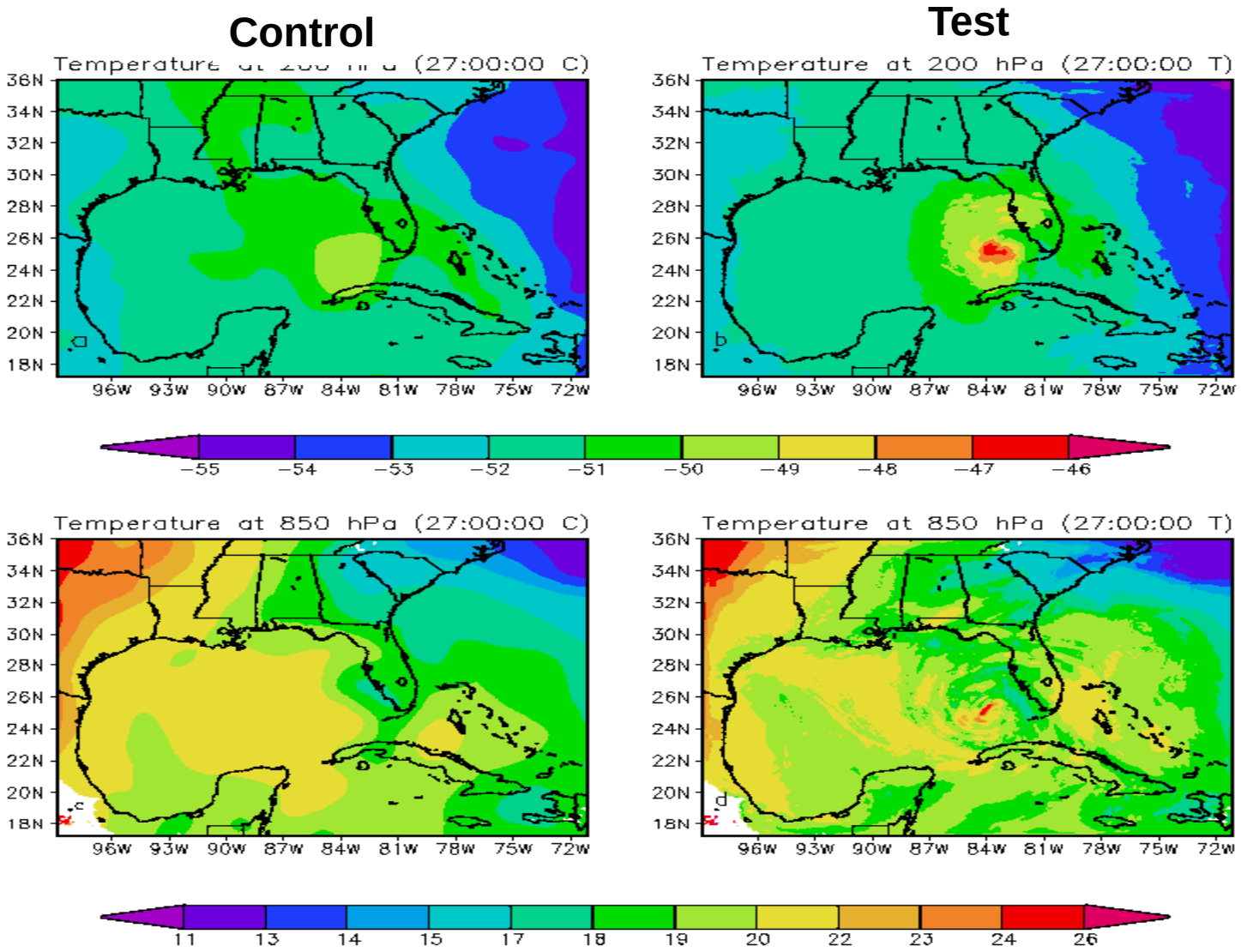

Liu and Weng, GRL, 2007

National Environmental Satellite, Data, and Information Service

Katrina Warm Core Evolution

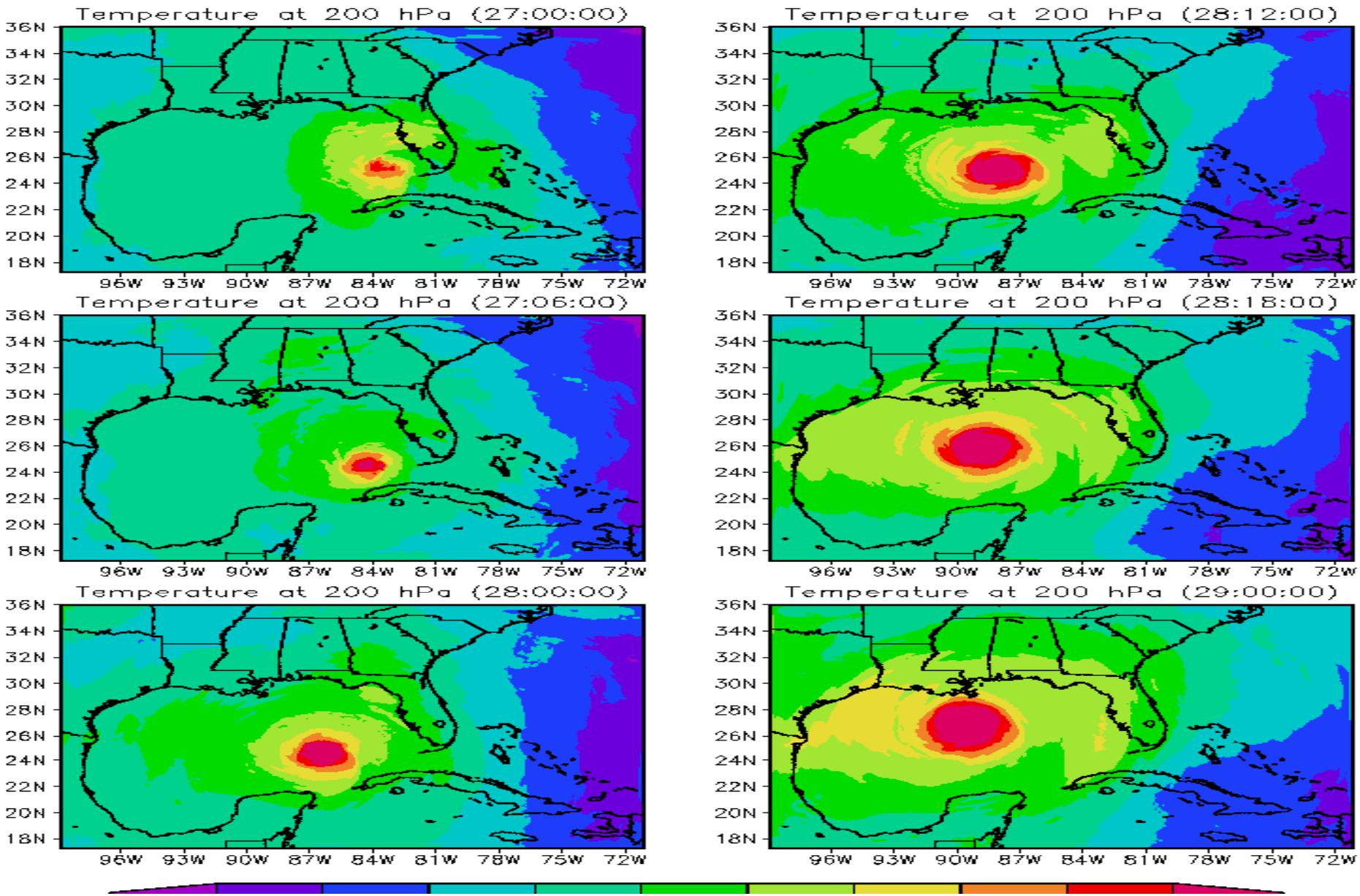

National Environmental Satellite, Data, and Information Service

Cloud Ice and Precipitation Distribution Hurricane Dean (2007)

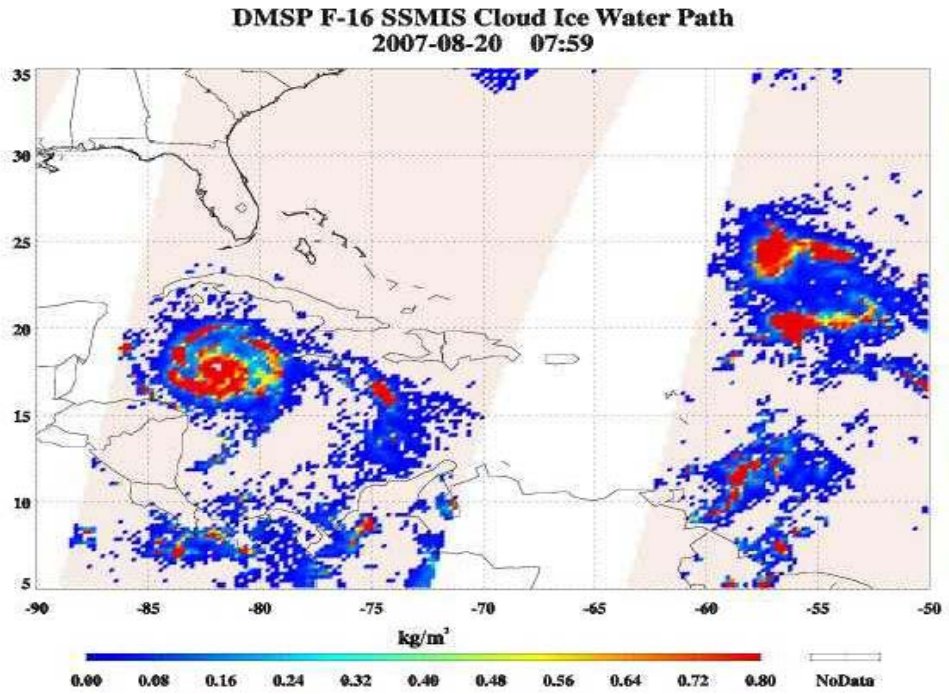

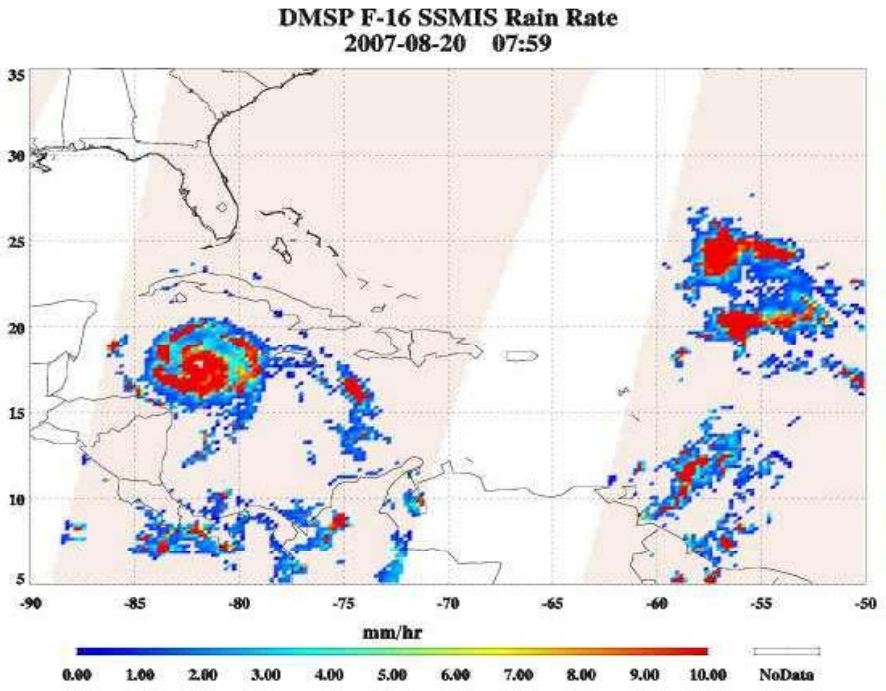

SSMIS Rain Rate Retrieval Algorithm Summary:

1. **Derive IWP and De from SSMIS 91 an 150 GHz using two-stream model (Weng and Grody, 2000)**
2. **IWP is then converted to surface rain rate (Weng et al., 2002)**
3. **SSMIS derived surface snow and sea ice is used to screen the false signature**

National Environmental Satellite, Data, and Information Service

Typhoon Luosha

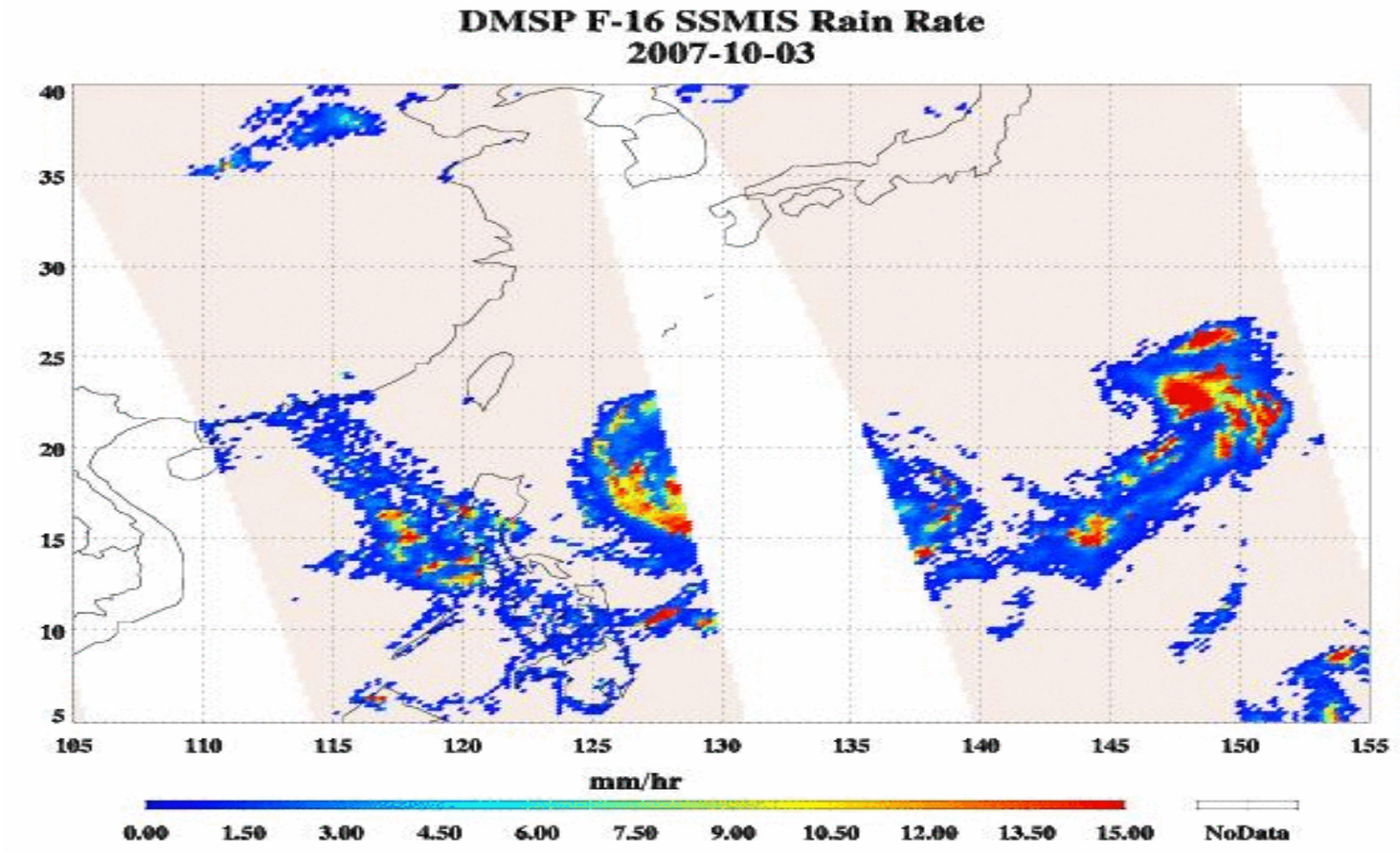

2008 IOWA Flooding

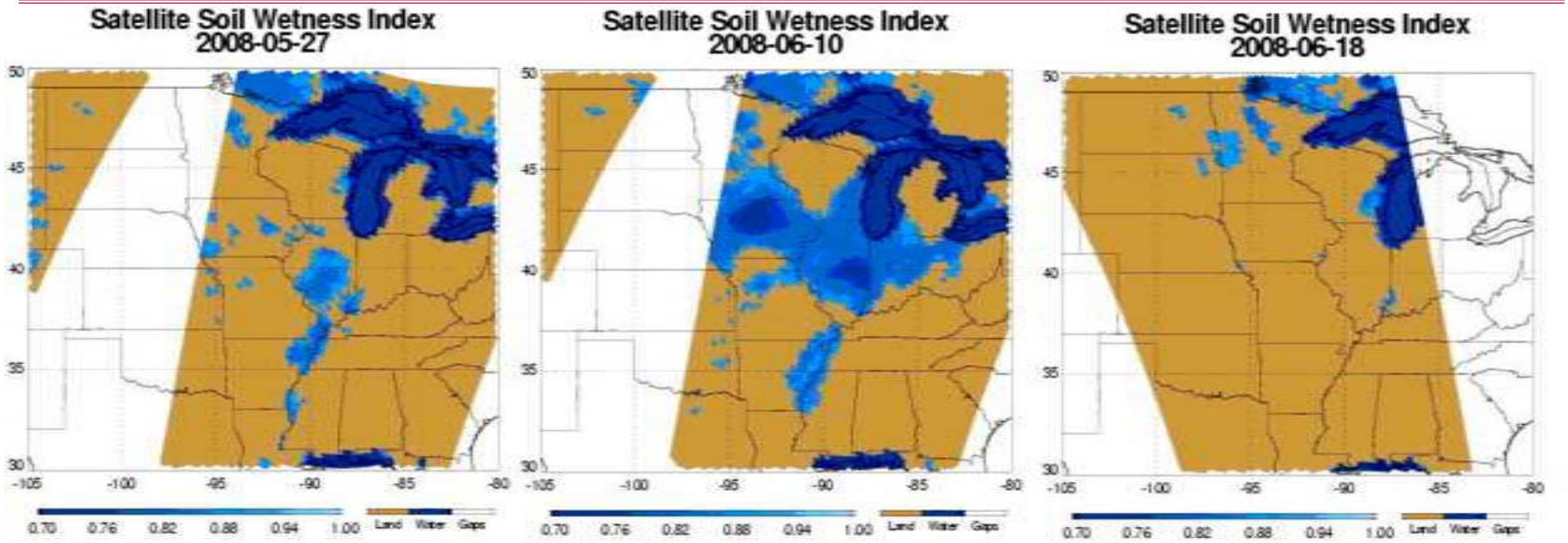

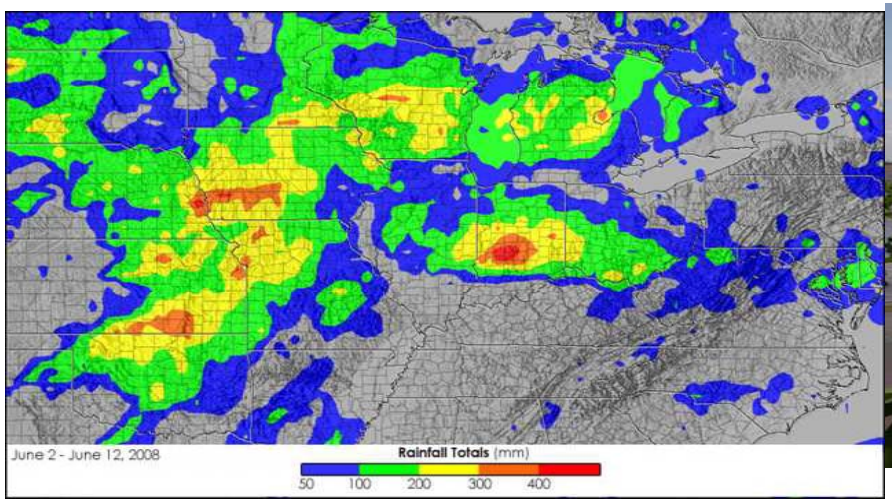

Summary

1. **Sounding and Imaging:**
   - Profiling atmosphere and imaging clouds, precip and surface
2. **Microwave Absorption Bands**:
   - O2 (50-60 Ghz, 117-120 GHz),
   - H2O (176-190 GHz)
   - Channels near the line centers for sounding
   - Channels between the lines for imaging
3. **Microwave Cloud Algorithms:**
   - Emission: cloud liquid water/total precipitable water
   - Scattering: ice water path/ particle size
4. **Microwave Sounding Algorithms**:
   - simultaneous retrievals from 1dvar
   - All weather profiling requires scattering rt model
   - Accurate surface emissivity model
5. **Main Applications**:
   - NWP data assimilations
   - Hurricane monitoring
   - Surface flooding